T.C.

BAHCESEHIR UNIVERSITY

GRADUATE SCHOOL

MECHATRONICS ENGINEERING HEAD OF THE DEPARTMENT

SEMI-ACTIVE SUSPENSION CONTROL DESIGN AND ANALYSIS FOR DIFFERENT TYPES OF VEHICLES AND ROAD IRREGULARITIES

MASTER'S THESIS

MERTCAN TEZCAN

ISTANBUL 2024

T.C.

BAHCESEHIR UNIVERSITY

GRADUATE SCHOOL

MECHATRONICS ENGINEERING HEAD OF THE DEPARTMENT

SEMI-ACTIVE SUSPENSION CONTROL DESIGN AND ANALYSIS FOR DIFFERENT TYPES OF VEHICLES AND ROAD IRREGULARITIES

MASTER'S THESIS

THESIS ADVISOR

ASST. PROF. BARAN ALİKOÇ

ISTANBUL 2024

T.C.

BAHCESEHIR UNIVERSITY

GRADUATE SCHOOL

MASTER THESIS APPROVAL FORM

Program Name:	MECHATRONICS ENGINEERING (ENGLISH, THESIS)
Student's Name and Surname:	Mertcan TEZCAN
Name of the Thesis:	Semi-active suspension control design and analysis for different types of vehicles and road irregularities.
Thesis Defense Date:	

This thesis has been approved by the Graduate School which has fulfilled the necessary conditions as Master thesis.

Assoc. Prof. Yücel Batu SALMAN

Institute Director

This thesis was read by us, quality and content as a Master's thesis has been seen and accepted as sufficient.

	Title/Name	**Institution**	**Signature**
Thesis Advisor's	Asst. Prof. Baran Alikoç	Graduate School	
Member's	Assoc. Prof. Mehmet Berke Gür	Graduate School	
Member's	Asst. Prof. Beste Bahçeci	Graduate School	

I hereby declare that all information in this document has been obtained and presented in accordance with academic rules and ethical conduct. I also declare that, as required by these rules and conduct, I have fully cited and referenced all material and results that are not original to this work.

Name, Last Name: Mertcan TEZCAN

Signature:

ABSTRACT

Semi-active suspension control design and analysis for different types of vehicles and road irregularities.

Mertcan, TEZCAN
Master's Program in Mechatronics Engineering
Supervisor: Asst. Prof. Baran ALİKOÇ

May 2024, 73 pages

Suspension design and ride comfort evaluation is conducted in this thesis. First, a suitable suspension kinematic setup and its controllers are investigated by considering a tradeoff between cost and efficiency. After a literature survey, it is decided to use semi-active MR damper suspension setup with on/off and continuous skyhook controls. MATLAB/Simulink and AVL VSM vehicle simulation tools are used to obtain vehicle models and see the behavior of the semi-active on/off and continuous skyhook-controlled vehicle suspension under two types of road irregularities for two vehicle types. The particle swarm optimization method is adapted to optimize the suspension parameters according to the root mean square of chassis acceleration. The optimal suspension parametrization is done for both vehicle types driven in case of considered road scenarios over simulations with Simulink. The suspension systems with the optimal controls are implemented in AVL VSM to assess the control performance comparison. As a result, there are several outcomes provided which we think they contribute to the literature. Achieving the best ride comfort depends on the simulation-based optimization which considers parametrization based on the road scenario. Moreover, natural absorbing capabilities of tire and suspension kinematics are required to be considered in suspension design. The semiactive controllers have different performances when applied different types of vehicles. This is shown by comparing the improvement results on the ride comfort as the scope of this thesis.

Key Words: Suspension Control, Skyhook Continuous Control, Semi-Active On/Off Control, Particle Swarm Optimization, Vehicle Simulation

ÖZ

Farklı araç ve yol düzensizlikleri için yarı aktif süspansiyon kontrol tasarımı ve analizi

Mertcan, Tezcan
Mekatronik Mühendisliği Yüksek Lisans Programı
Tez Danışmanı: Asst. Prof. Baran ALİKOÇ

May 2024, 73 sayfa

Bu tezde süspansiyon tasarımı ve sürüş konforu değerlendirmesi yapılmıştır. İlk olarak, maliyet ve verimlilik dikkate alınarak uygun bir süspansiyon kinematik kurulumu ve kontrolcüleri araştırılmıştır. Literatür taramasından sonra, on/off ve skyhook sürekli kontrolcülere sahip yarı aktif MR süspansiyon kurulumunun kullanılmasına karar verilmiştir. MATLAB/Simulink ve AVL VSM, araç modelleri elde etmek ve iki araç tipi için iki tip yol düzensizliği altında yarı aktif on/off ve skyhook sürekli kontrollü araç süspansiyonunun davranışını görmek için kullanılmıştır. Parçacık sürüsü optimizasyon yöntemi, şasi ivmelenmesinin ortalama karekköküne göre süspansiyon parametrelerini optimize etmek için uyarlanmıştır. MATLAB/Simulink ile yapılan simülasyonlar üzerinden, dikkate alınan yol senaryolarında sürülen her iki araç tipi için optimum süspansiyon parametrelendirmesi yapılmıştır. Optimum kontrollere sahip süspansiyon sistemleri, kontrol performansı karşılaştırmasını değerlendirmek için AVL VSM'de uygulanmıştır. Sonuç olarak, literatüre katkıda bulunacağını düşündüğümüz birkaç sonuç sağlanmıştır. En iyi sürüş konforuna ulaşmak, yol senaryosuna dayalı parametrelendirmeyi dikkate alan simülasyon tabanlı optimizasyona bağlıdır. Ayrıca, lastiğin doğal sönümleme kabiliyetlerinin ve süspansiyon kinematiğinin süspansiyon tasarımında dikkate alınması gerekir. Yarı aktif kontrolcüler farklı araç tiplerine uygulandığında farklı performanslara sahiptir. Bu, bu tezin kapsamı olarak sürüş konforundaki iyileştirme sonuçlarının karşılaştırılmasıyla gösterilmiştir.

Anahtar Kelimeler: Süspansiyon Kontrolü, Skyhook Sürekli Kontrol, Yarı Aktif On/Off Kontrol, Parçacık Sürü Optimizasyonu, Araç Simülasyonu

Dedicating

ACKNOWLEDGEMENTS

I wish to express my deepest gratitude to my supervisor Asst. Prof. Baran Alikoç for his guidance, advice, criticism, encouragements, and insight throughout the research.

I would also like to thank my parents, Hayati TEZCAN and Gül TEZCAN and my sister Mercan TEZCAN, for their great support throughout my life. Without their understanding, and continuous support, I could have never been able to aspire for this level of education and complete this study.

TABLE OF CONTENTS

LIST OF TABLES

TABLES

LIST OF FIGURES

FIGURES

Chapter 1

Introduction

Automotive industry has been investing a considerable amount of money and effort to develop suspension systems due to several reasons. First, customers are always demanding better ride comfort and handling performances from the vehicle in terms of safety and comfort (Allied Market Research, 2023). Secondly, to prevent the harming effects of vibration to human body. Finally, original equipment manufacturers (OEMs) are always willing to increase their reputations among the customers (OEM Off-Highway, 2024)

Increased handling and ride comfort have a direct impact on vehicle safety (Salmani, Abbasi, Fahimi Zand, Fard, & Nakhaie Jazar, 2022). The likelihood of crashes and accidents is decreased by responsive steering and smooth handling, which improve driver control and manoeuvrability. Similarly, enhanced comfort during the ride lessens driver weariness, enhancing awareness and reaction times when driving. In fact, long trips are made more pleasurable and driver stress is decreased by a smooth ride and responsive handling. Moreover, vibration negatively affects the human body, especially if they are experienced strongly or repeatedly. Musculoskeletal conditions like neck discomfort, joint stiffness, and lower back pain can result from prolonged vibration exposure, particularly whole-body vibrations (Dacova, 2021). On the other hand, ride comfort and handling characteristics of a vehicle have a direct impact on manufacturer reputation. Good feedback and word-of-mouth recommendations about a vehicle's performance and comfort level increase customer satisfaction and brand loyalty, which boosts sales and market share (Kırbaş & Karaşahin, 2023).

To sum up, there are three suspension systems available on the mass market which are passive, semi-active, and active suspension which will be explained in Section 2. In fact, researchers are extensively working on these suspensions to enhance the vehicle due to the reasons given above.

1.1 Statement of the Problem

The automotive industry has faced with dramatically increasing amount of customer expectations in terms of ride comfort. Nowadays, ride comfort is not only an issue for just passenger vehicles but also a particular amount of ride comfort is expected even for commercial vehicles. On the other hand, cost is another issue which is required to be reduced in manufacturing. For that reason, engineering studies focus on increasing the ride comfort and meeting the customer expectations while decreasing the cost of the vehicles.

There are significant number of studies available in the literature which are related to suspension (Theunissen, Tota, Gruber, Dhaens, & Sorniotti, 2021). Some of these are discussing suspension kinematic arrangements on the vehicle, see e.g., (Genta & Morello, 2020) (Yang, Zang, Xu, Li, & Tan, 2023), while the others are proposing control strategies with suitable optimization techniques (Streiter, 2008) (Fukuda, Zhang, Hasegawa, Matsumoto, & Hoshino, 2004) (Savaresi & Silani, 2004). Moreover, developing spring, damper characteristics are also a field of study (Rusli & Darsivan, 2019). In fact, this huge and dramatically increasing customer expectations are trying to be met somehow by working strictly on automotive suspension. However, most of the suspension ride comfort studies are over linear models but, the application of designed suspension to real vehicles should also be investigated. Furthermore, different types of vehicles might have different reactions when they are exposed to same road irregularities. The reason behind this, each vehicle type has unique nonlinearities in their physical models which might directly or indirectly effect on the ride comfort unpredictably. In fact, even though the suspension controllers are the same, the performances might differ. Therefore, verification of the suspension design for each vehicle separately is a crucial issue. Besides, the road scenarios and the vehicle characteristics should also be considered thoroughly while determining the suspension control parameters due to same reasons.

This study focuses on addressing these issues described in the above paragraph by implementing an effective semi-active suspension control strategy and its parameter optimization over linear models for achieving simplified suspension design in terms

of the vehicle ride comfort for two types of vehicles driven on different road conditions. Then, the results gathered from linear models are applied to nonlinear vehicle dynamic models. for an accurate performance investigation in increasing ride comfort. In this way, it aims to support literature and shows significant simulation results which we think are valuable in suspension design.

1.2 Purpose of The Study

This thesis examines the ride comfort evaluation by considering the chassis vertical acceleration of commercial and compact class passenger vehicles. Moreover, we parametrize the selected semi-active suspension control laws via a simulation-based optimization to achieve an optimum ride comfort in terms of the vertical chassis acceleration. The control parametrization is done through two road scenarios, namely while the vehicle is crossing over a standard speed bumper and is driven on a standard (ISO 8608) road profile. Also, we consider the semi-active suspension control of two different types of vehicles. One is a passenger compact class, and the other one is a light duty commercial vehicle. One of the purposes of the study is to see the real time dynamic behaviour of these vehicles by implementing the suspension designed over simplified versions of the vehicle dynamic models. To do this, effective and simply executable suspension control methodologies are selected to optimize the trade-off between engineering effort and suspension performance improvement. Another purpose is to compare the performance of the determined controls with passive suspension for different road conditions and for different type of vehicles. Also, this work compares the performance improvements for two different types of vehicles after implementation of determined control laws with determined suspension control parameters for achieving all of these purposes, verified nonlinear models provided by a commercial tool is used and compared with the widely used linear simplified models.

Chapter 2

Literature Review

Automotive suspension systems are designed to enhance dynamic behaviour of the vehicle. Main functionality of the suspension systems are as follows (Theunissen, Tota, Gruber, Dhaens, & Sorniotti, 2021):

- Providing vehicle stability by arranging the vehicle body roll and pitch orientation under braking, traction, and cornering forces
- Dissipating road irregularities and providing ride comfort to the occupants.
- Providing road handling and vehicle safety by reducing the wheel load fluctuations subjected to random road irregularities.
- Preventing excessive wheel travel and successively absorb the impact when vehicle crossing bumpers.

For achieving these objectives listed above, independent, and dependent suspension systems are used in automotive applications.

2.1 Dependent Suspension

In the kinematics of dependent suspension, the vertical dynamic behaviour of one wheel on an axle directly effects the other wheel on the same axle. Indeed, when one wheel encounters a bump or irregularity in the road surface, the movement of the suspension compresses or extends the axle, causing the other wheel on the same axle to move in the same direction. This brings poor ride quality and handling capability when it is compared with independent suspension. On the other hand, because of their simple design and cost effectiveness, they are used in some automotive applications especially the vehicles where ruggedness, simplicity, and cost-effectiveness are priorities such as off-road vehicles, utility vehicles, and trucks (Rajamani, 2012).

2.2 Independent Suspension

In the kinematics of independent suspension system, each wheel is typically connected to the vehicle's chassis through its own set of suspension components. In fact, the vertical movement of each wheel do not directly affect to each other. This independence of movement helps to improve vehicle stability, handling, and ride comfort by reducing the transfer of forces between wheels when it is compared with dependent suspension applications. Moreover, independent suspension systems are suitable for tuning (optimizing) applications. Tuning the suspension parameters with a trade-off among handling, comfort, and safety is possible. Therefore, independent suspensions are widely used in performance-oriented vehicles such as compact class passenger cars, SUVs, crossovers (Rajamani, 2012) (Kaldas, Caliskan, Henze, & Küçükay, 2014).

Road holding and occupant comfort conflict to each other in the suspension system. If the optimization on road holding is achieved, the vehicle often subjected to high amount of vertical frequency which causes poor ride comfort. On the other hand, if the optimization on comfort is achieved, this causes reducing in vibration, but causes poor vehicle stability especially while turning corners. This conflict between road holding and comfort is shown in *Figure 1*. For this reason, performance trade-off must be considered to optimize vehicle suspension system (Ahmadian, 2001) (De Bruyne, Van der Auweraer, Anthonis, Desmet, & Swevers, 2012).

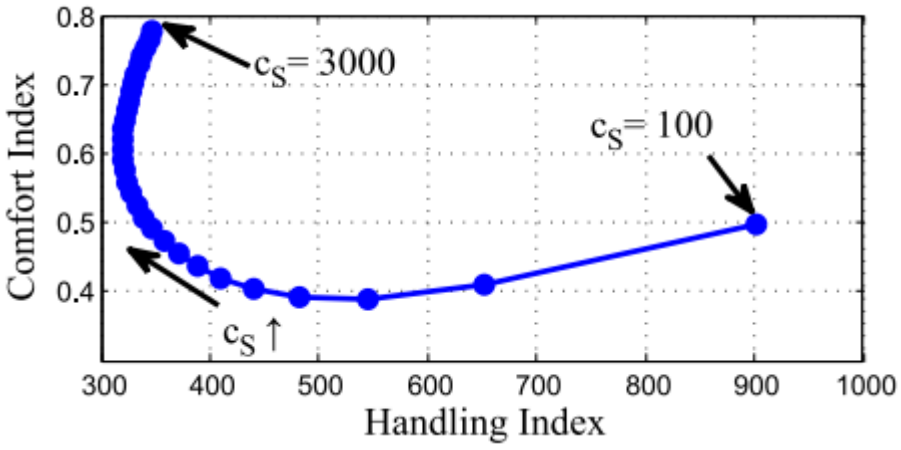

Figure 1 Passive suspension system comfort and handling index conflict diagram.

2.2.1. Suspension types. A passive suspension system damping and spring ratios are determined during suspension design stage. Trade-off between handling and comfort is also assigned in this stage. Basically, according to the intended application and deterministic goals, suspensions can store energy thanks to springs and dissipating energy thanks to characteristics of damper. However, most of the vehicles are driven on different road conditions. Therefore, needs on comfort or road handling is highly dependent on the type of the road condition. Passive suspension system does not have ability to arrange this trade-off according to changing road conditions (Ahmadian, 2001) (De Bruyne, Van der Auweraer, Anthonis, Desmet, & Swevers, 2012).

Arrangements of this trade-off continuously on varying road conditions can be achieved by implementing controlled suspension systems on the vehicle. The controlled suspension is realized by replacing passive suspension damping parameter with semi-active and/or active actuators (Theunissen, Tota, Gruber, Dhaens, & Sorniotti, 2021).

In semi-active suspension systems, damping actuators has variable force speed characteristics according to changing road properties. Generated force by semi-active dampers always opposes the actuator motion. However, these features of semi-active dampers have major drawbacks in vehicle dynamics point of view. The ride height and the roll angle in cornering as well as the pitch angle induced during longitudinal acceleration performances of semi-active damper actuators have limitations. On the other hand, the energy required to run the hardware of semi-active suspension actuator is considerably low. In fact, semi-active actuators consume power when only adjusting their control mechanisms. This means they don't directly contribute to generating force but rather modulate existing forces. Consequently, the energy consumption of the vehicle isn't significantly affected by the operation of semi-active actuators, as their power usage is primarily limited to the adjustment process rather than continuous force generation (Theunissen, Tota, Gruber, Dhaens, & Sorniotti, 2021).

Widely used semi-active actuators are listed below:

- Electrohydraulic (EH) dampers
- Magnetorheological (MR) and electrorheological (ER) dampers:

- Electromagnetic (EM) dampers

In the EH dampers, solenoid valves located inside or outside of the actuators are controlled by changing the size of the orifices so that the damping ratio changes continuously (Savaresi, Poussot-Vassal, Spelta, Sename, & Dugard, 2010).

In the MR and ER dampers, a piston cylinder assembly filled with non-Newtonian characteristics of fluid provides different viscous properties when exposed to magnetic or electrical fields. The simplified version of a typical MR damper system layout and its physical assembly is illustrated in *Figure 2* and *Figure 3*, respectively (Theunissen, Tota, Gruber, Dhaens, & Sorniotti, 2021). In Figure 2, F_d is the force generated by the damper; i_{cmd} is the commanded current generated by the control algorithm; i_c is the coil current which acts to change the damping ratio of the damper and u_c is the supply voltage applied to the magnetic circuit within the control valve of the MR damper (Gołdasz & Dzierzek, 2016).

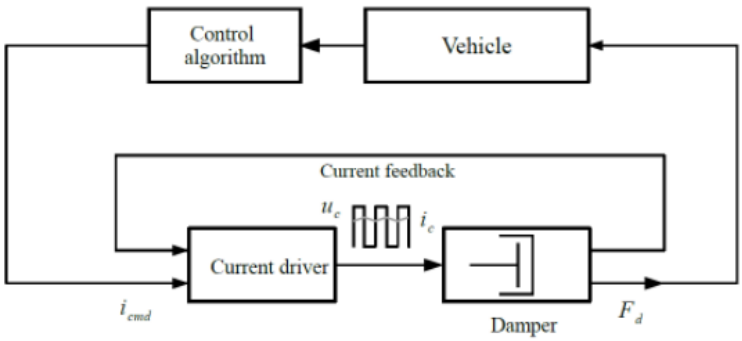

Figure 2 MR damper system layout (simplified version).

In the EM dampers, damping effect is provided by movement of the coil and the permanent magnet. Damping coefficient is altered by changing external resistance. When the coil is shortened to its minimum length, the damping coefficient reaches its maximum value. Conversely, when the coil is extended to its maximum length, the damping coefficient reaches its minimum value. Moreover, the strength of the magnetic field also affects the damping characteristics. As the magnetic field increases, the damping ratio decreases or vice versa. Some of the pictorial representation of EM dampers are shown in *Figure 4* (Soliman & Kaldas, 2021).

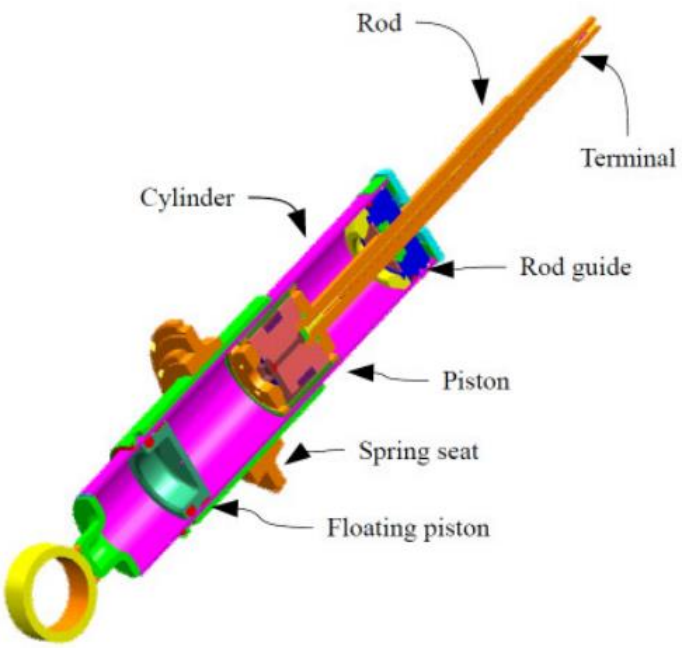

Figure 3 Automotive single-tube MR damper.

Figure 4 From left to right: solenoid valve EH damper from Sachs, MR damper from Delphi and ER damper from Fludicon.

In active suspension systems, the direction of the actuator force is independent of the sign (direction) of the actuator speed. Because of its independence, the system can be adjusted for various vehicle motions such as roll, pitch and heave motions brought on by lateral and longitudinal accelerations. Furthermore, active suspension systems can adjust the vehicle's ride height. For instance, they may lower the car during fast-moving situations to minimize the energy loss and the aerodynamic drag. Besides that, active suspension systems do have several disadvantages, even though they offer better performance. A high amount of power input is needed to generate the positive

mechanical effort needed to actively adjust the suspension. Power conversion devices, e.g. electric motors or hydraulic pumps must be used as a result. The additional energy used by these parts affects the vehicle's overall energy consumption. As a result, even while active suspension systems provide enhanced ride quality and sophisticated control capabilities, their application necessitates carefully weighing the trade-offs between efficiency and performance (Theunissen, Tota, Gruber, Dhaens, & Sorniotti, 2021).

Mostly used active suspension actuators are as follows:

- Hydraulic actuators
- Electro – magnetic actuators
- Electro - mechanical actuators

The hydraulic actuators which are consisting of an actuator, primary power spool valve and a secondary bypass valve are driven with electrohydraulic system. This system generates a mechanical force between sprung and unsprung masses as seen in *Figure 5*. With matching and symmetric orifices, the hydraulic actuator cylinder is positioned in a follower configuration to an electrohydraulic power spool valve that is critically cantered. High pressure fluid flow is directed to one of the cylinder chambers by positioning the spool u_1, which also links the other chamber to the pump reservoir. A pressure differential P_L is produced across the piston by this flow. The active force F_A for the suspension system is determined by multiplying this pressure difference by the piston area A_p (Sam & Hudha, 2006).

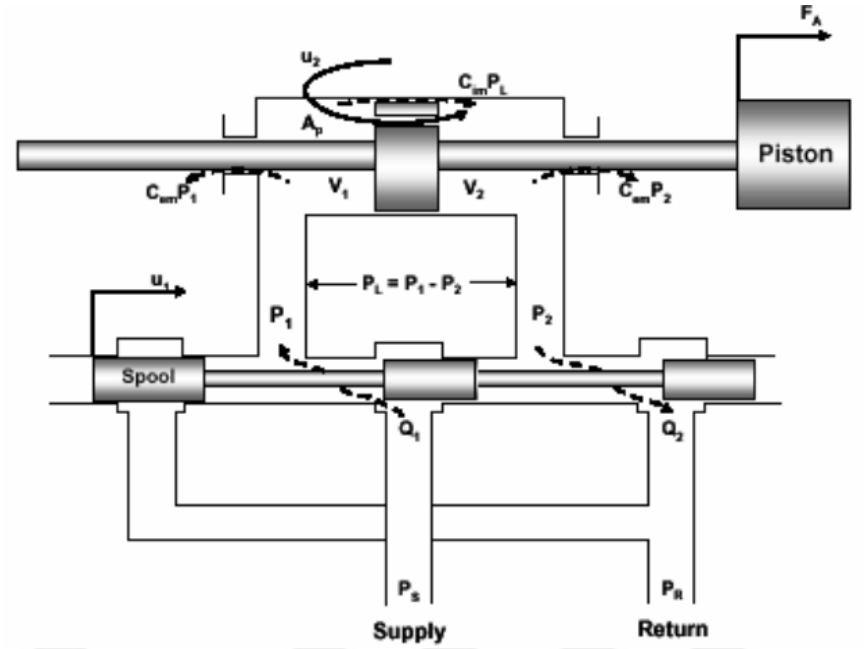

Figure 5 Physical schematic and variables for the hydraulic actuator.

The working principle of electromagnetic actuators are almost the same with electromagnetic dampers which are discussed above. On the other hand, electromechanical actuators use induced current which is converted to mechanical force. They are commonly used in active suspension system applications. Basically, the system consists of nut ball screw and motor assembly, which is demonstrated in *Figure 6* (Song & Wang, 2020).

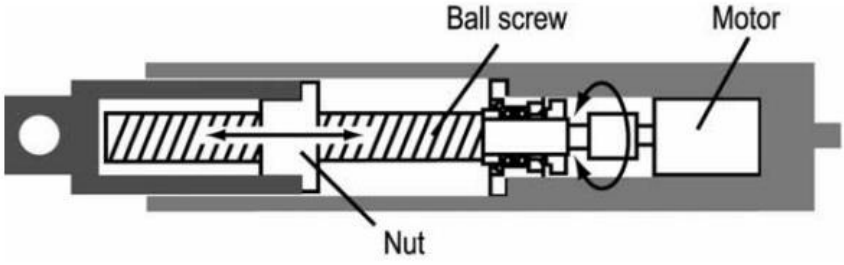

Figure 6 Concept of electromechanical actuator.

2.2.2. Suspension control methods. There are several approaches to control semi-active and active suspension actuators mentioned above (Kaldas, Caliskan, Henze, & Küçükay, 2014) (Chen, He, Liu, & Yao, 2012) (ElMadany & Abduljabbar, 1999) (Sharkawy, 2005) (Skogestad & Postlethwaite, 2005). These control strategies are designed to offer an adaptable suspension solution that maximizes handling, stability, and ride comfort under a variety of driving conditions and preferences. For achieving this objective, these actuators dynamically modify the damping characteristics of the suspension system to enhance vehicle stability and ride handling performance by getting feedback from sensors that measure various vehicle-ride and handling signals. These sensors are capable of continuously monitoring vehicle speed, sprung and unsprung masses' acceleration and road conditions. In this way, controlled suspension helps to minimize body roll, improve traction, and grip, and enhance overall stability and road handling during cornering, braking, and acceleration manoeuvres. Research and development efforts in semi-active and active suspension focus on refining and optimizing these systems to achieve better stability and handling characteristics for vehicles. Some practical applications have been introduced to realize the mentioned objectives (Theunissen, Tota, Gruber, Dhaens, & Sorniotti, 2021) (Soliman & Kaldas, 2021) (Mo & Sunwoo, 2002).

A variety of practical applications have been developed to optimize vehicle performance and ride quality. Skyhook control, for instance, firstly introduced by Karnopp (Karnopp & Crosby, 1974) focuses on minimizing vertical acceleration of the vehicle body in relation to the road surface by simulating an ideal suspension point above the vehicle. The name of the concept comes from the notion of a "skyhook" which vehicle chassis remains stationary in relation to the road surface and a fictional point in the "sky" (Yang, Zang, Xu, Li, & Tan, 2023).

On the other hand, the Groundhook control aims to replicate the behavior of an ideal passive damper system that is "hooked" between the tire and the ground (Liu, Chen, Lee, Yang, & Zhang, 2023). In practical, the Groundhook suspension adjusts the damping coefficient of the suspension system based on real-time feedback from sensors that measure tire displacement relative to the road surface.

In both Skyhook and Groundhook approaches which are shown in *Figure 7*, the goal is to simulate an idealized suspension point, either above the vehicle (skyhook) or connected to the road surface (groundhook), that remains stationary relative to the vehicle or road. However, achieving the perfect Skyhook or Groundhook in practical implementations are not possible. Therefore, the ideal Skyhook or Groundhook behavior must be closely approximated by control algorithms and suspension systems (Liu, Chen, Lee, Yang, & Zhang, 2023) (Liu, Chen, Yang, Zhang, & Yang, 2019).

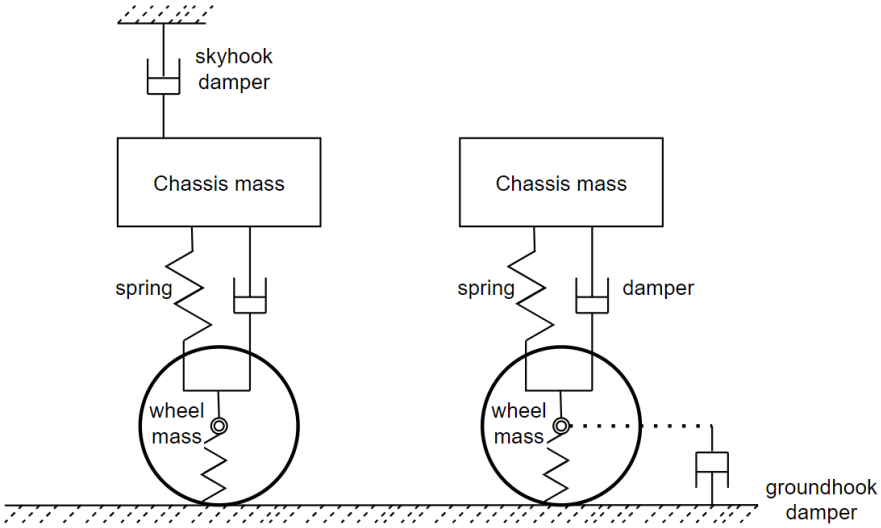

Figure 7 (a) Skyhook model, (b) Groundhook model.

There are several control methods available in the literature for both semi-active and active suspensions; one can see (Drehmer, Paucar Casas, & Gomes, 2015) (Shihabudheen, Mahesh, & Pillai, 2018) (Wang, Lv, & Li, 2015) for a comprehensive review. Model predictive control (MPC) is one of the well-known methods to optimize semi-active actuator damping coefficient. Morato et al. claims (Morato, Nguyen, Sename, & Dugard, 2019) that dissipative constraints are one of the key factors in controlling semi-active actuators. The term "dissipative" describes the damper's capacity to disperse energy, which is essential for both stable driving and efficient vibration control. The actuator saturation problem provides an approach to treat the dissipative limitations of dampers to address these constraints within the MPC framework. Actuator saturation is referred when the damping coefficient reaches its maximum or minimum limits and cannot be adjusted further. Through the integration of the dissipative constraints as actuator saturation limits in the MPC optimization

problem, the controller can efficiently control the damping coefficient within the allowable range, guaranteeing that the semi-active damper function is within their desired limits. Furthermore, Song and Wang suggests (Song & Wang, 2020) to apply an incremental MPC approach for active suspension systems, along with a road profile estimator which makes use of preview data from a lead vehicle. Two scaled-down active suspension stations are used to empirically evaluate the effectiveness of the suggested technique in relation to two traditional active suspension control methods.

Rossi and Lucente study the control of semi-active suspensions by using H_∞ state-space optimization approaches (Rossi & Lucente, 2004). They created the quarter car and half car standard variants of the system, each having three H_∞ controllers in the fully active scenario. Then, these controllers are modified utilizing a type of H_∞ clipped control to fit the nonlinear real system. While the second controller concentrated on enhancing both comfort and handling, the first controller sought to maximize ride comfort. A global controller based on the half-car concept is the third controller. To assess the suggested controllers, performance metrics pertaining to ride comfort and driving safety were created. The study's findings demonstrated that, in comparison to a passive model, the controls offered better ride comfort. The variables pertaining to unsprung mass dynamics might also be included to the error signals vector to improve drive safety performances. Comparing the semi-active controlled suspensions to the passive settings, the simulations showed that the former produced greater levels of ride comfort and safe drive. Furthermore, (Sharp & Peng, 2011) discusses in their paper the application of optimal control theory on semi active and active controlled suspension designs under the worst-case maneuvering. Similarly, (Savaresi & Silani, 2004) works on optimal predictive control theory, and they compare the controller performances for comfort-oriented semi active suspension. (ElMadany & Abduljabbar, 1999) work on frequency domain for designing multivariable controllers. They use quarter car model to implement intelligent controlled suspension.

2.2.3. Performance index. Researchers frequently use metrics which are based on established standards such as ISO 2631-1 (1997) and BS 6841 (1987) to evaluate human exposure to whole-body vibrations (ISO 2631-1:1997, 1997) (BS 6841:1987, n.d.). Although the vertical acceleration of the sprung mass is the focus of many investigations, other factors such as the displacement of the sprung mass or jerk which is the derivative of acceleration over time, are also looked at. An uncomplicated way of assessing suspension performance, especially in response to isolated road events, is to compute the peak or peak-to-peak values of these variables over a predetermined measurement interval. Finding the frequency weighted root mean square (WRMS) acceleration is a common way to improve this assessment approach as it provides a more comprehensive analysis of ride comfort and vibration exposure. As an alternative method to WRMS, some of the research uses root mean square (RMS) of acceleration values which are derived from 1/3 octave frequency bands. Furtherly, there are also other approaches used as ride comfort metrics which are the running weighted RMS acceleration (RWRMS), the maximum transient vibration value (MTVV) and the fourth power vibration dose (VDV) (Theunissen, Tota, Gruber, Dhaens, & Sorniotti, 2021).

2.2.4. Optimization methods. In the literature, there are several methods to optimize vehicle suspension parameters to reduce the trade-off between road handling and ride comfort. A class of stochastic global search and optimization techniques known as genetic algorithms (GAs) are motivated by the ideas of natural biological evolution, namely Charles Darwin's "survival of the fittest" theory. These algorithms look for optimal or nearly optimal solutions within a search space by iteratively evolving and improving possible answers to optimization issues. Yu and Yu use GA to determine stiffness and damping coefficients of the suspension (Yu & Yu, 2003). Furthermore, Drehmer et al. utilize the sequential quadratic programming techniques and Particle Swarm Optimization (PSO) to determine the ideal suspension parameters for various road profiles and vehicle velocities (Drehmer, Paucar Casas, & Gomes, 2015). This way, the desired performance curves given in ISO 2631 about the weighted limits for vertical acceleration at the driver’s seat, road holding of the vehicle and bump-stop and rebound limits (suspension working space) of suspension are achieved.

To solve optimization problems, Kennedy and Eberhart developed PSO method in 1995 (Kennedy & Eberhart, 1995) (Drehmer, Paucar Casas, & Gomes, 2015). It has been used in a variety of fields, e.g. for machine learning for neuro-fuzzy systems and vehicle trajectory design (Zhuo, Cheng, Wang, & Liu, 2018) (Shihabudheen, Mahesh, & Pillai, 2018) and for enhancing the passive suspension performance (Wang, Lv, & Li, 2015). Additionally, several studies are available in the literature which use PSO methodology for ride comfort evaluation. Zhang (2024) proposes optimal fuzzy PID active control strategy by implementing PSO algorithm. The aim is to improve ride comfort for transverse leaf spring suspension for commercial vehicles (Zhang, Long, Lin, & Zhu, 2024). Moreover, Tharehalli mata, (2021) works on quarter car vehicle dynamic model and an optimal sliding mode controller (SMC) which is optimized by PSO to determine the parameters for SMC in terms of ride comfort (Tharehalli Mata, Mokenapalli, & Krishna, 2021). Different aspect from the literature, we use PSO approach to optimize the semi-active suspension control parameters over linear Matlab/Simulink models for each considered scenario and vehicle type. Then, the parameters are applied to nonlinear AVL VSM vehicle models to see the real-world behavior and improvements on the vehicle ride comfort. This way, the applicability of the found parameters via PSO through simplified linear simulation models is verified by their application to validated VSM full car dynamic models. Also, differently from the literature, the PSO algorithm is implemented for non-identical suspension setups for the light duty vehicle where the suspension spring and damping coefficient limits differ for the front and rear axles.

Chapter 3

Vehicle Dynamic Models

3.1 Quarter Car Model

Vertical dynamic behaviour of the chassis is often analysed with simplified version of the vehicle dynamic models. Quarter car models are representing one corner of the vehicle. Chassis mass, wheel masses are considered quarterly. Quarter car models are very effective especially while evaluating ride comfort on dedicated road profiles. The main drawback which affects the accuracy of this model is due the lacking consideration of the pitch and roll motion of the vehicle. This model does not capture full complexity of real-world vehicle dynamic behaviour caused by inertia in the longitudinal direction of the vehicle. The 2 degree of freedom (DOF) quarter car model which is considered in this study is illustrated in *Figure 8* consisting of the following elements:

- Sprung mass (M_s) which represents quarter mass of the vehicle chassis.
- Unsprung mass (M_u) which represents the wheel and the suspension mass of the vehicle.
- Suspension spring element with the stiffness coefficient (K_s)
- Wheel spring element with the stiffness coefficient (K_w)
- Suspension damper element with the damping coefficient (C_s)

The quantities z_s and z_u in *Figure 8* represent the displacements of the sprung and unsprung mass from their central point, respectively, whereas z_r stands for the distance from the tire bottom point to the road. The model is constructed on two bodies which are sprung and unsprung masses that accounts for two independent directions of motion, i.e. 2-DOF.

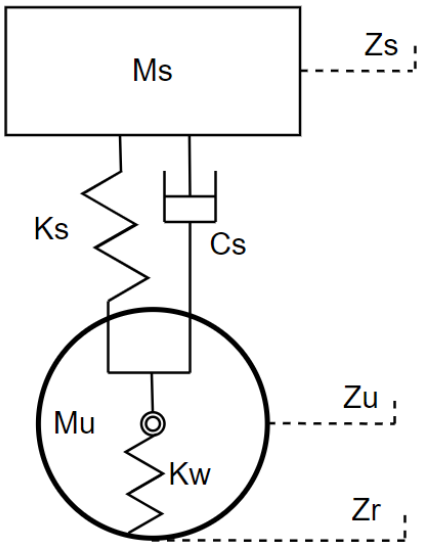

Figure 8 Quarter car passive suspension model.

The following equations of motion expressed in Eq. (1) are used to describe the vertical dynamic behaviour of the passive quarter car vehicle suspension system (Rajamani, 2012):

$$\ddot{z}_s = \frac{1}{m_s}[k_s(z_s - z_u) + c_s(\dot{z}_s - \dot{z}_u)]$$

$$\ddot{z}_u = \frac{1}{m_u}[k_s(z_u - z_s) + c_s(\dot{z}_u - \dot{z}_s) + k_w(z_r - z_u)] \quad \text{Eq. 1}$$

3.2 Half Car Model

Quarter car models are only used for observing vertical vehicle dynamic behaviour of the vehicle. The vehicle dynamic behaviour resulting from the roll and pith motions can be investigated by using a half car vehicle model which is demonstrated in *Figure 9* where the sub-index *f* stands for 'front', *r* stands for *'rear', cog* stands for 'centre of gravity', I_y is the pitch axis moment of inertia, M_s is the half of the mass of the chassis, θ is the pitch angle. In this study, we consider the simplified bicycle model which acts for the longitudinal cross section of a vehicle to examine the effect of pitch motion on the vehicle's vertical dynamic behaviour (Rajamani, 2012).

The geometric relationship of the pitch motion is described as follows:

$$z_{s,f} = z_{s,cog} + l_f \sin(\theta)$$

$$z_{s,r} = z_{s,cog} - l_r \sin(\theta)$$

$$\dot{z}_{s,f} = \dot{z}_{s,cog} + l_f \dot{\theta} \cos(\theta) \qquad \text{Eq. 2}$$

$$\dot{z}_{s,r} = \dot{z}_{s,cog} - l_r \dot{\theta} \cos(\theta)$$

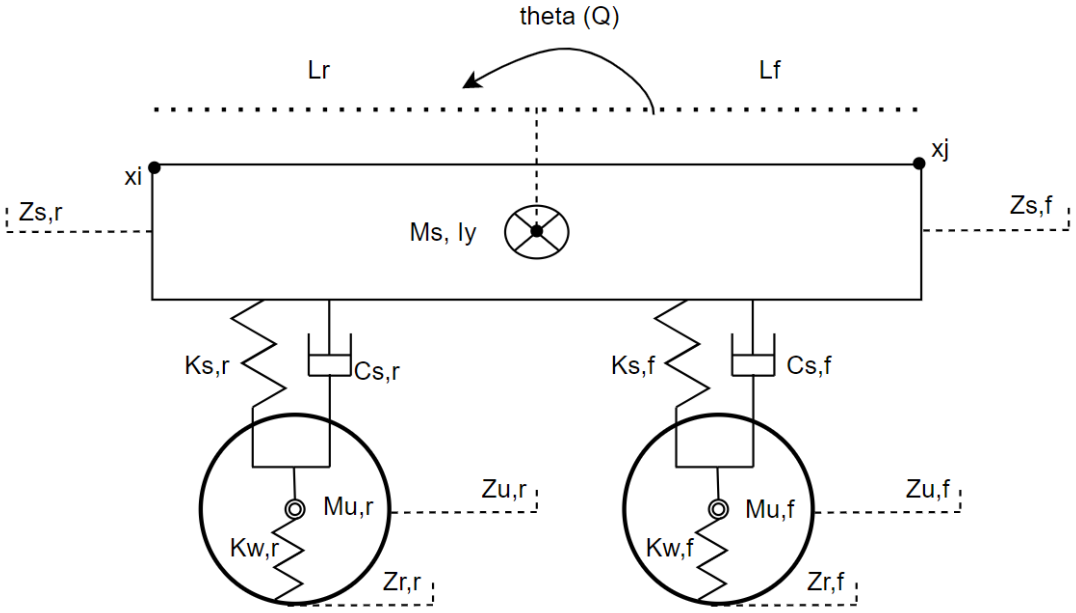

Figure 9 Half car passive suspension model.

The following equations of motion given in Eq. (3) are used to describe the vertical behaviour of the passive half car vehicle suspension system (Rajamani, 2012).

$$\ddot{z}_{s,cog} = \frac{1}{m_{s,cog}}[-(l_f\theta + z_{s,cog} - z_{u,f})k_{sf} + (l_r\theta - z_{s,cog} + z_{u,r})k_{sr} - (l_f\dot{\theta} + \dot{z}_{s,cog} - \dot{z}_{s,f})c_{sf} + (l_r\dot{\theta} - \dot{z}_{s,cog} + \dot{z}_{s,r})c_{sr}$$

$$\ddot{\theta} = \frac{1}{I_{yy}}[-l_f(l_f\theta + z_{s,cog} - z_{u,f})ks_f - l_r(l_r\theta - z_{s,cog} + z_{u,f})k_{sr} - l_f(l_f\dot{\theta} + \dot{z}_{s,cog} - \dot{z}_{s,r})c_{sf} - l_r(l_r\dot{\theta} - \dot{z}_{s,cog} + \dot{z}_{s,r})c_{sr} \qquad \text{Eq. 3}$$

$$\ddot{z}_f = \frac{1}{m_f}[(l_f\theta + z_{s,cog} - z_{u,f})k_{sf} + (l_f\dot{\theta} + \dot{z}_{s,cog} - \dot{z}_{s,f})c_{fs} - (z_f - z_{r,f})k_{wf}$$

$$\ddot{z}_r = \frac{1}{m_r}[-(l_r\theta - z_{s,cog} + z_{u,r})k_{sr} - (l_r\dot{\theta} - \dot{z}_{s,cog} + \dot{z}_{s,r})c_{rs} - (z_r - z_{r,r})k_{wr}$$

3.3 Full Car Model

Full car vehicle models are used in the literature to simulate and analyse the vehicle dynamic behaviour in various aspects. A full car model enables to evaluate and optimize the handling, ride comfort and acceleration & deceleration behaviour of the vehicle in a more accurate way. Yun et al. use 7-DOF full car vehicle model which is shown in Figure 10. In this vehicle model, m_s stands for the sprung mass, m_f stands for each of front wheel unsprung mass and m_r for each of rear wheel unsprung mass, k_f-k_r are the front-rear suspension stiffness coefficients, c_f-c_r are the front-rear suspension damping ratios and anti-roll bar K_f for 'front axes' and K_r for 'rear axes' are used. The motion of unsprung masses is defined with z_1, z_2, z_3 and z_4 . The COG position is determined at a distance of l_1, l_2 and w_1, w_2. The motion of chassis (sprung mass) is described with the vertical displacement (Z) from the COG point. The pitch and roll angles are denoted by ϕ and θ, respectively. The sprung mass has the mass moment of inertia about the x-axis and y-axis denoted by I_x and I_y, respectively. The centrifugal force applied to vehicle at distance h from the roll axis is denoted by M_r (Yun, Lee, Jang, Kim, Choi, & Chung, 2023).

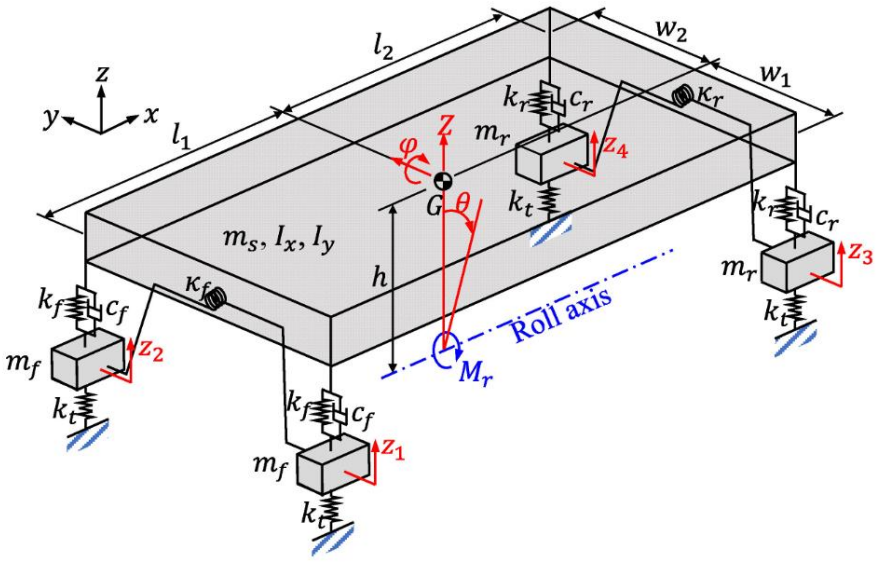

Figure 10 7-DOF full car vehicle model.

The relationships between vehicle components are established by the full car vehicle dynamic model, which enables precise behaviour prediction of the vehicle under various driving conditions. Full car vehicle dynamic models can be implemented and analysed using simulation tools like MATLAB/Simulink, CarSim, and Adams. In this study, a commercial tool by AVL company which is explained in the following section is used to simulate suspension behaviour on the full car model.

3.3.1 Vehicle simulation and modelling (VSM) tool. Individual elements of complex systems are commonly isolated from each other and analysed separately to simplify the models. However, such simplifications cause inaccurate simulations as compared to the real vehicle behaviour in a complete manner. The Vehicle Simulation and Modelling (VSM) tool produced by AVL company provides a dynamic simulation tool to realize the whole behaviour of the vehicle under different road conditions. AVL VSM offers validated default model setups for different types of vehicles. Vehicle static geometry setup, vehicle subsystem dynamic arrangements such as steering, braking, tyre, suspension, traction units and aerodynamic setup can be utilized in VSM. As a result of this, longitudinal, lateral, and vertical dynamic behaviour of the vehicle can be observed and analysed (AVL, 2021). In the following sections, we introduce the necessary setups and features of VSM tool which we use for the vehicle suspension simulations to analyse the performance of passive and semi-active suspension control.

3.3.1.1 Vehicle Geometry setup. The following cartesian coordinate system for a vehicle, which is illustrated in Figure 11, is used as default in AVL VSM (AVL, 2021):

X: Vehicle longitudinal direction (+X – vehicle is moving forward)
Y: Vehicle lateral direction (+Y – vehicle moving left)
Z: Vehicle vertical direction (+Z – vehicle moving up/skywards)
Accordingly, the rotations around these axes are defined as follows:
Roll [φ]: Rotation around X-axis (+φ – vehicle in roll)
Pitch [θ]: Rotation around Y-axis (+θ – vehicle decelerating)
Yaw [ψ]: Rotation around Z-axis (+ψ – vehicle in yaw)

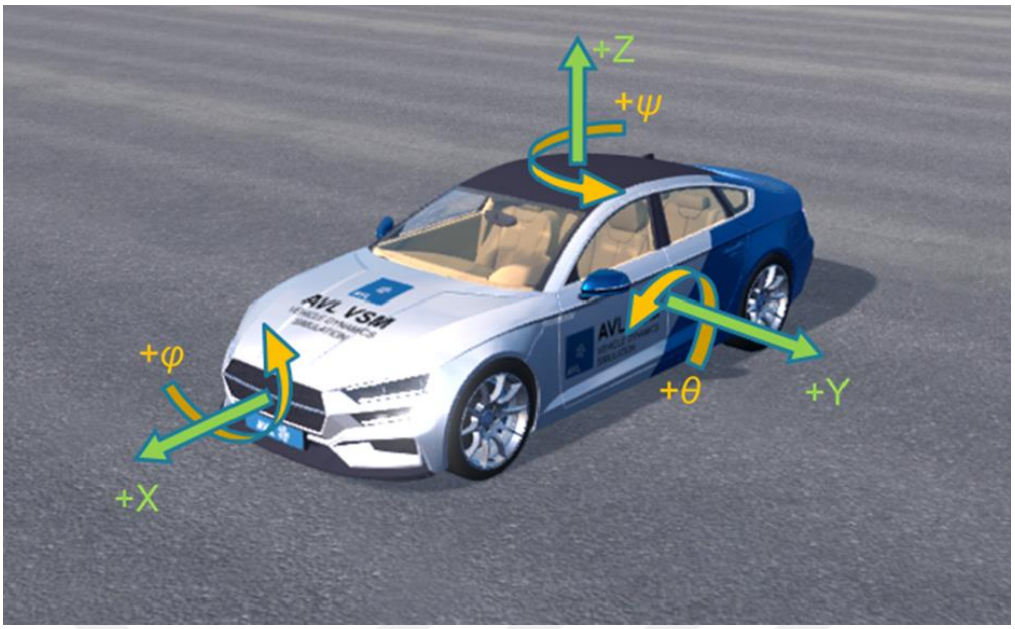

Figure 11 Default coordinate systems used in AVL VSM.

The static parameters of the vehicle such as the vehicle distribution, centre of gravity (COG) position, torsional stiffness, and inertias of X-, Y-, and Z- axis, vehicle, and the driver masses seen in *Figure 12* can also be determined. In fact, the asymmetric ballast can be achieved by using these facilities of the VSM. The vertical distance between COG and ground defines the COG height. The COG position and height is determined considering both the sprung and unsprung masses. The 'Wheelbase' is the longitudinal distance between centre of front and rear axles. The 'Wheel Track' is the lateral distance between wheel centres (AVL, 2021).

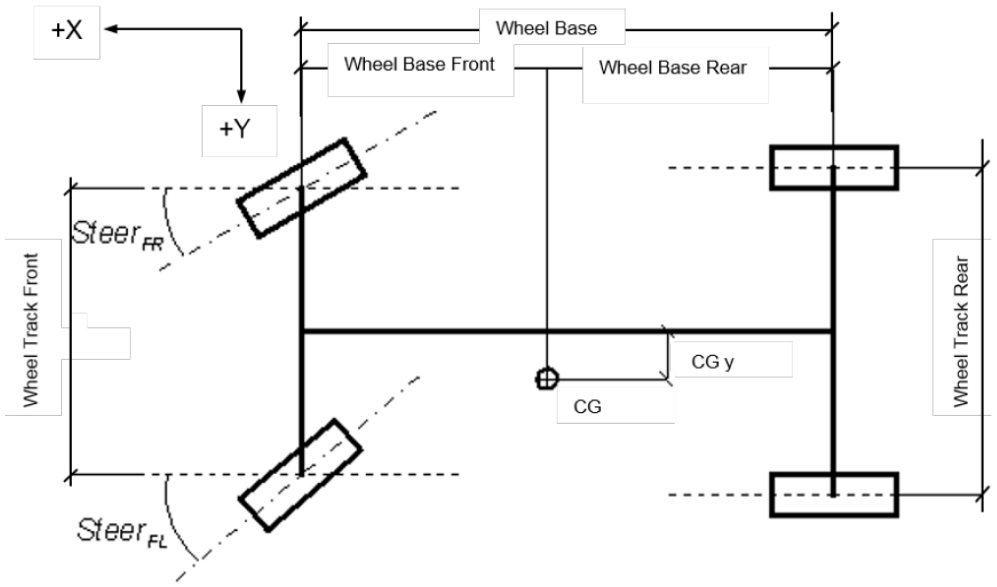

Figure 12 Illustration of vehicle geometry parameters.

3.3.1.2 Suspension front/rear setup. The vertical position of the chassis relative to the wheels can be arranged in suspension kinematics. Delta camber is one of the kinematic parameters defined to realize suspension's vertical effect on ride comfort. Delta camber angle seen in Figure 13 is directly related with the ride height changes and the track width. It is defined as the vertical tilt of the wheels from the vertical plane. If a wheel is tilted out, it is called as positive camber and vice versa if the wheel is tilted in (AVL, 2021).

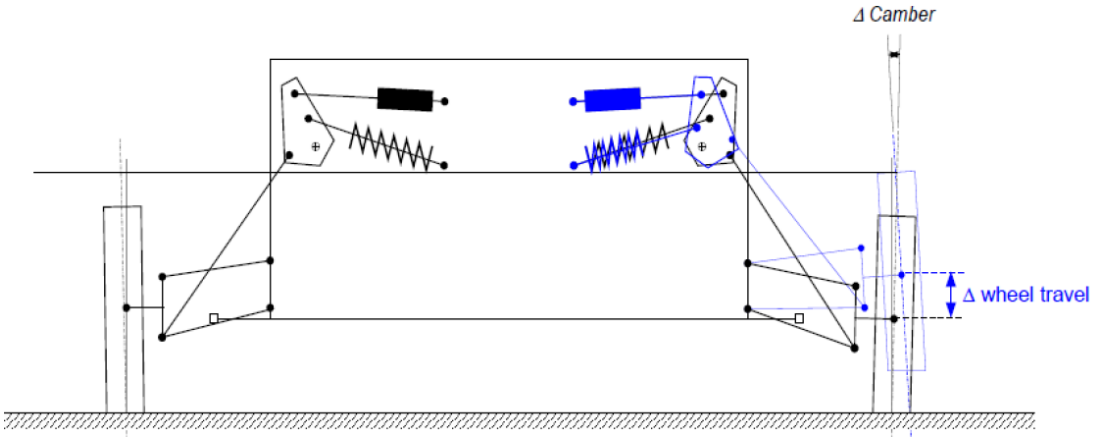

Figure 13 Delta camber due to ride height change.

Besides the camber there are several other important suspension static arrangement parameters available for directional stability of the vehicle in different

road conditions. Kingpin inclination demonstrated in *Figure 14* is another important parameter which is defined as the vertical inclination of vehicle suspension from the vertical axis of wheels (AVL, 2021).

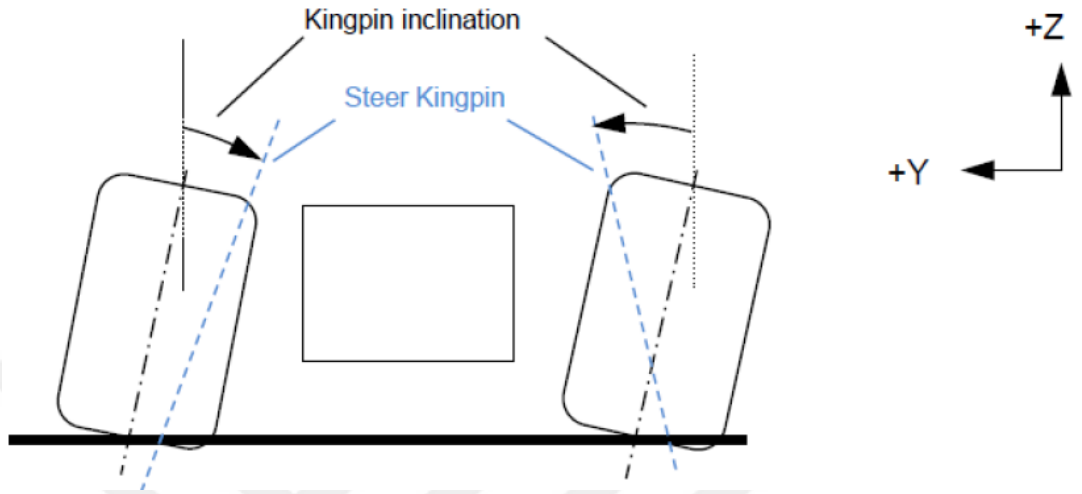

Figure 14 Definition of kingpin inclination.

Moreover, the scrub radius seen in *Figure 15* is defined as the lateral distance between the contact patch and the point where the steering kingpin axis intersects the ground. The scrub radius is positive, if the kingpin axis intersects the ground inside of the contact patch (AVL, 2021).

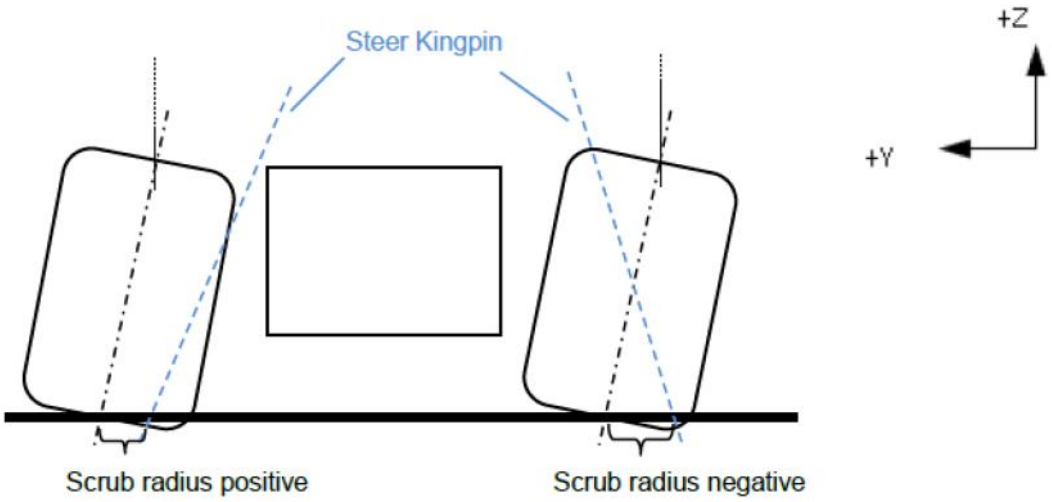

Figure 15 Definition of scrub radius.

The longitudinal distance between the contact patch and the ground plane intersection of the steering kingpin axis is known as the static mechanical trail that is seen in *Figure 16*. In case the steer kingpin crosses the ground before the contact patch, the mechanical trail will be positive. The mechanical trail is therefore negative if the steer kingpin crosses the ground behind the contact patch (AVL, 2021).

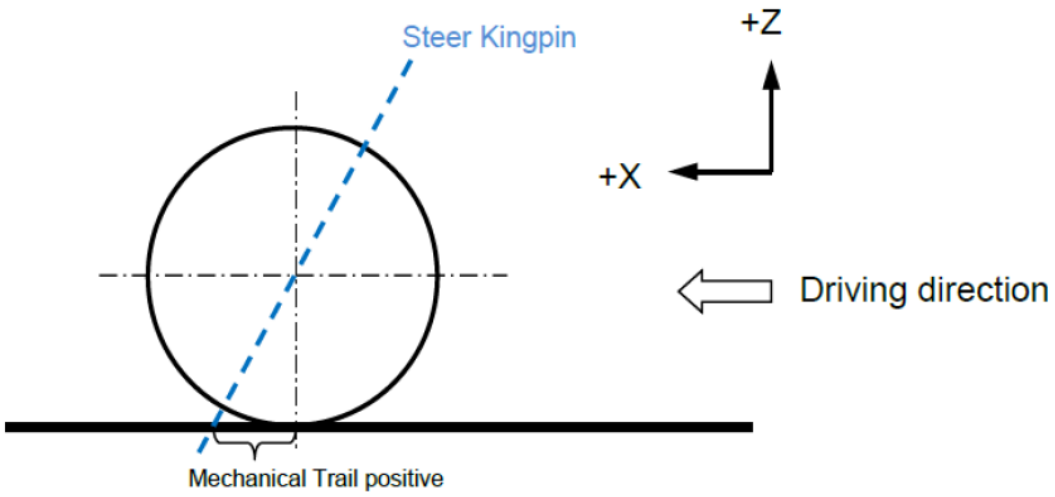

Figure 16 Definition of mechanical trail.

These suspension kinematic arrangements explained above are used to investigate the controller effects in nonlinear model environment. On the other hand, tyre setup as a physical implementation can also be utilized to enhance the suspension for ride comfort. It is possible to define different characteristics for each tyre. The coordinate system used in tyre setup in VSM environment is shown in *Figure 17* (AVL, 2021).

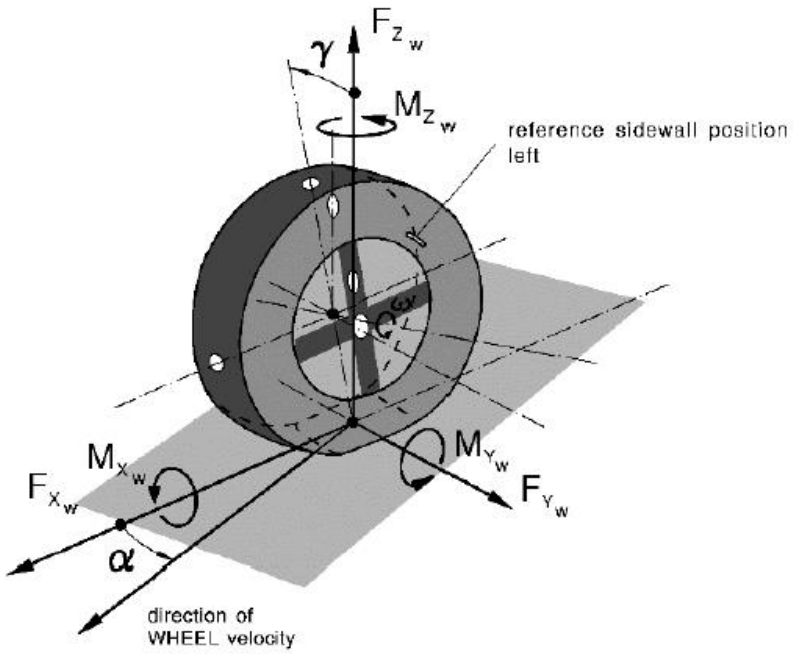

Figure 17 Tyre ordinate directions.

The nonlinear tyre parameters considerably affect the vehicle suspension performance and therefore the ride comfort. The tyre coefficient, the vertical wheel load and the wheel camber are the inputs to determine the potential tyre force map (AVL, 2021).

The spring and damper parameters can be given with nonlinearities in VSM. There are two spring selection mode available in VSM which are coil and torsion spring. Moreover, the force maps of the springs and dampers can be determined. The spring characteristics are defined with a map with the spring compression versus the spring force in coil spring. Similarly, damping characteristics of the suspension is determined with a damping force map. The damper compliance which means the stiffness between the dampers and the wheels can be considered for the ride comfort evaluation (AVL, 2021).

The spring and damper which are the sub elements of a suspension work within the rebound and the bump stop limits. The illustration given in *Figure 18* explains these suspension intervention limits in a real vehicle (AVL, 2021).

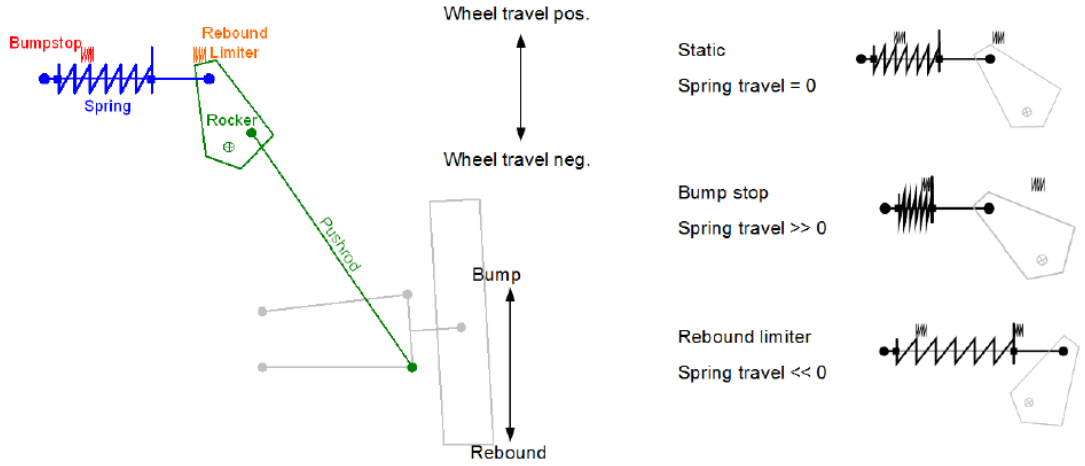

Figure 18 Definition of bump and rebound and the respective travels.

To sum up, the kinematic and the dynamic parameters of the suspension systems on a vehicle has significant effects on the vehicle ride comfort. The nonlinear characteristics of the vehicle and suspension dynamics, which are not usually considered in quarter and half car models in the literature, are important to simulate the overall behaviour of the vehicle and correspondingly the performance analysis of suspension systems. To investigate such effects, we consider the comparison of widely used suspension control techniques over the simulations based on the quarter car, the half car and the VSM full car model (AVL, 2021).

Chapter 4

Vehicle Suspension Control and Simulation Models

4.1 Passive Suspension

Dynamic parameters of a passive suspension system which are sprung, unsprung masses, tyre and suspension stiffness coefficients and damping coefficient are defined, and the quarter and half car models are created in Simulink environment considering Eq. (1-3) expressed in Chapter 3. The constant suspension spring coefficient is selected based on the VSM vehicle parameters for a compact class C-segment Sedan car and a light duty VAN electric vehicle (EV). Moreover, the suspension damping coefficients are obtained from this VSM default vehicle models regarding the force maps of the dampers shown in *Figure 19*, *Figure 20* and *Figure 21*. The nonlinearities in the force maps are neglected for simplification and the constant mean value is selected to be used in the models. This selection is done due to analyse the refined effect of the considered suspension controls explained in the following sections. Notice that the suspension damping characteristics of the VAN EV are different for the front and the rear axles whereas they are identical for the compact Sedan car. This difference in VAN EV causes an additional fact to the vertical dynamics of the vehicle so that the parametrization of the suspension control is done differently as compared to the Sedan car which will be explained in the relevant chapter (AVL, 2021).

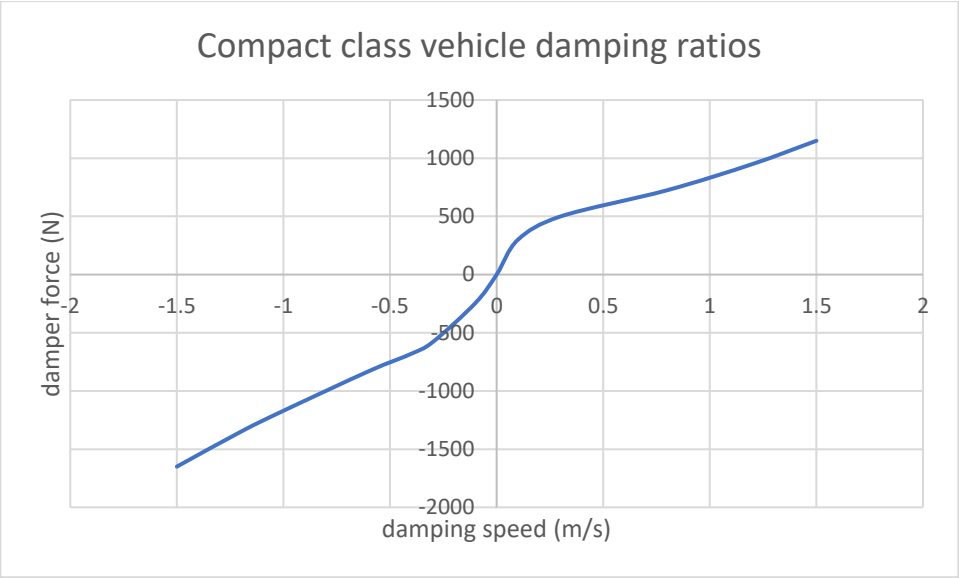

Figure 19 Compact Sedan vehicle nonlinear damping coefficients.

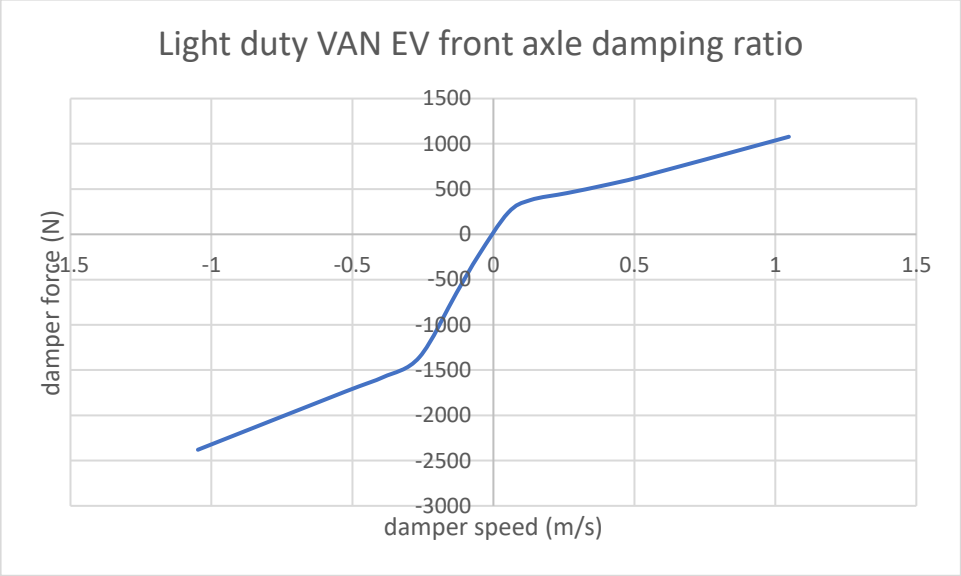

Figure 20 VAN EV front axle nonlinear damping coefficients.

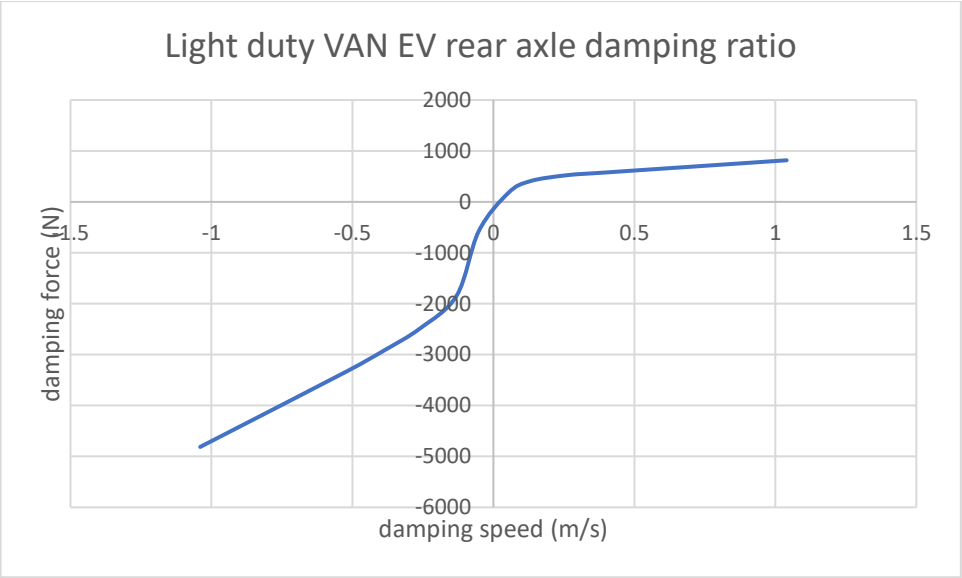

Figure 21 VAN EV rear axle nonlinear damping coefficients.

The quarter and half car and VSM full var Simulink models with passive suspension are provided in Appendix A, B and C in the last section.

4.2 Semi-active Suspension

Semi-active controllers which are on/off and skyhook continuous are designed by using MATLAB Simulink environment. To achieve this objective, mathematic expressions which are expressed in below section are used. In fact, they are implemented to previously created car models. Simulink models of these controllers are represented in Appendix E and F.

4.2.1 Semi-active on/off suspension control. In the semi-active on/off suspension system control, according to road input there are two selectable damping ratios are offered to the system based on the difference between the acceleration of sprung and unsprung masses.

The control algorithm is working with a simple logic where the damper coefficient is changed from its minimum value to maximum value or vice versa. In other words, if the relative velocity between sprung mass and unsprung mass is equal to or smaller than zero, the minimum value of the damping coefficient is applied to the

system and the corresponding force is generated by the damper. On the other hand, if the relative velocity between sprung and unsprung mass is greater than zero, the maximum damping coefficient is applied to generate the maximum force. Thus, the control law of semi-active on/off suspension is given as (Soliman & Kaldas, 2021):

$$c_{s,sa} = c_{s,sa\_max} = \dot{z}_s(\dot{z}_s - \dot{z}_u) > 0$$
$$c_{s,sa} = c_{s,sa\_min} = \dot{z}_s(\dot{z}_s - \dot{z}_u) \leq 0 \qquad \text{Eq. 4}$$

The suspension control law in Eq. (4) is realized in Simulink as presented in Appendix E. For determining the minimum and maximum damping coefficients in Eq. (4), the PSO algorithm (cf. Section 4.3) is used according to RMS value of the sprung mass acceleration. The main objective is to make sprung mass acceleration as smallest as possible. For doing this, RMS value of sprung mass acceleration is calculated as follows (Theunissen, Tota, Gruber, Dhaens, & Sorniotti, 2021):

$$RMS = \sqrt{\frac{1}{n}\sum_i \dot{z}_i} \qquad \text{Eq. 5}$$

The sprung mass acceleration data is collected from MATLAB/Simulink environment. Then, the PSO algorithm is used to determine the minimum and maximum damping values of the suspension control which minimizes the cost function given by Eq. (4) to improve the ride comfort.

4.2.2 Semi-active skyhook continuous suspension. The "skyhook" concept brings up an explanatory picture in which the sprung mass is joined to an imaginary hook in the sky as seen in Figure 22 by means of a fictive damper $\boldsymbol{C_{sky,sa}}$. Without limiting wheel movements, this hypothetical damper would create a force that resists the vertical motions of the vehicle sprung mass body. The intention is to reduce the body's reaction to road inputs and dips in the road by considering in a fictional manner that the vehicle's body is suspended from above.

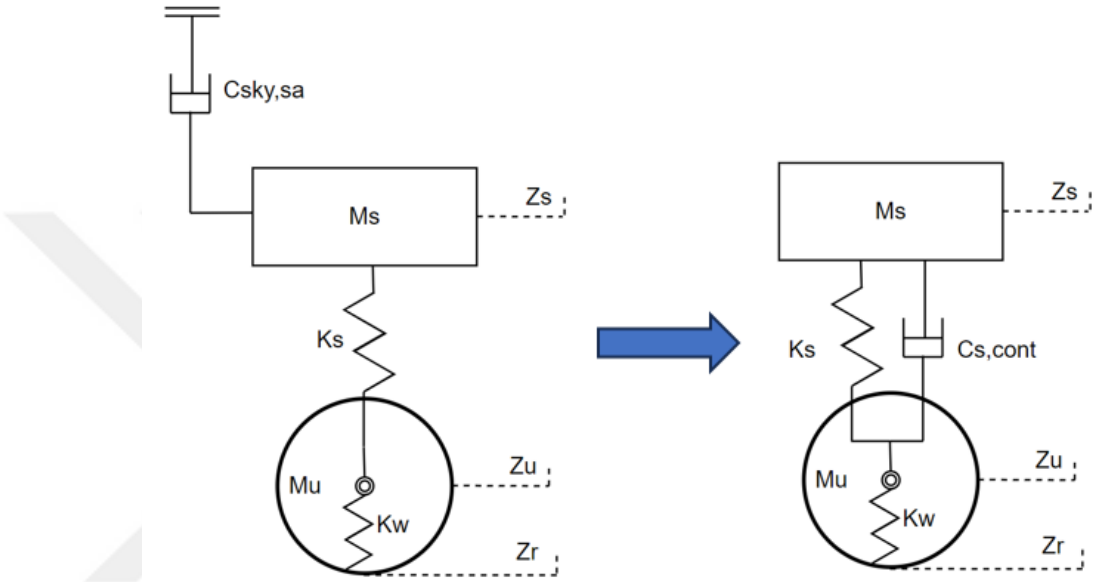

Figure 22 Skyhook semi-active suspension system

For this purpose, the relative velocity between the sprung and unsprung masses

$$\dot{Z}_{su} = \dot{Z}_s - \dot{Z}_u \qquad \text{Eq. 6}$$

is considered (Soliman & Kaldas, 2021).

The skyhook force applied to sprung mass is needed to be determined. First assume that for both sprung and unsprung masses is moving upwards, and the sprung mass velocity is greater than unsprung mass velocity. Then, the skyhook force applied to sprung mass is described in Eq. (7) below as follows:

$$F_{sky} = -c_{sky,sa}\dot{Z}_s \quad \text{Eq. 7}$$

Now, we need to identify whether the semi-active damper is able to generate the same force or not by considering the equation:

$$F_{cs,cont} = -C_{s,cont}\dot{Z}_{su} \quad \text{Eq. 8}$$

In fact, in skyhook theory, skyhook force applied sprung mass should be equal to force generated from the continuous force from opposite direction to keep sprung mass in ideal stationary case. Therefore, when Eq. (7) and Eq. (8) are considered, the following skyhook suspension damping coefficient is described (Liu, Chen, Yang, Zhang, & Yang, 2019):

$$C_{s,cont} = C_{sky}\frac{\dot{Z}_s}{\dot{Z}_{su}} \quad \text{Eq. 9}$$

since the same amount of force applied in opposite direction.

For determining the realized damping coefficient which is $C_{s,cont}$ theoretical damping coefficient which is C_{sky} should be obtained from ideal 2nd order system. In fact, the damper speed coefficient which is $\frac{\dot{Z}_s}{\dot{Z}_{su}}$and theoretical damping coefficient give realized damping coefficient. For doing this, the ideal 2nd order system is used as described in Eq. (10):

$$m\ddot{x}(t) + c\dot{x}(t) + kx(t) = 0 \quad \text{Eq. 10}$$

Laplace transform is applied to convert the system from time domain to frequency domain which is expressed as follows:

$$ms^2 + C_{sky}s + k = 0 \quad \text{Eq. 11}$$

Rearranging the equation Eq. (12) as

$$s^2 + \frac{C_{sky}}{m}s + \frac{k}{m} = 0, \qquad \text{Eq. 12}$$

the undamped natural frequency can be obtained as:

$$\omega_n = \sqrt{\frac{k}{m}} \qquad \text{Eq. 13}$$

Then, C_{sky} is determined from

$$\frac{C_{sky}}{m} = 2\zeta\omega_n \qquad \text{Eq. 14}$$

where ζ is the damping ratio of the ideal system. For achieving a desired trade-off between frequency and resonance, ζ value is determined as 0.707 as illustrated in *Figure 23* (Alciatore & Histand, 2012).

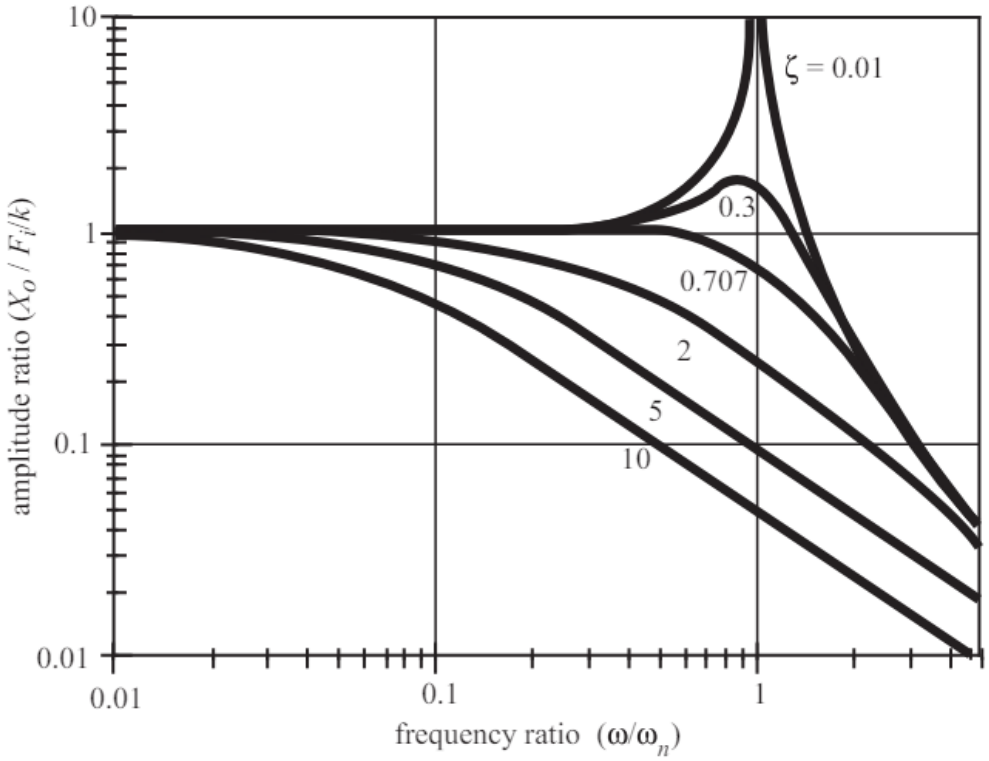

Figure 23 2nd order system damping ratios.

The skyhook continuous control law enables the damping coefficient of the suspension is always varying according to the sprung mass acceleration. Unlike the semi-active on/off system, the skyhook continuous is expected to provide less sprung mass acceleration thanks to this variable damping ratio. This way, a better ride comfort can be achieved with the skyhook-controlled vehicle suspension (Liu, Chen, Yang, Zhang, & Yang, 2019).

The control algorithm is similar to the semi-active on/off control and described as:

$$c_{s,cont} = \max(c_{min}, \min\left(\frac{c_{sky}\dot{z}_s}{\dot{z}_s - \dot{z}_u}, c_{max}\right)), \qquad \dot{z}_s(\dot{z}_s - \dot{z}_u) \geq 0$$
$$c_{s,cont} = c_{min}, \qquad \dot{z}_s(\dot{z}_s - \dot{z}_u) < 0 \qquad \text{Eq. 15}$$

The minimum (c_{min}) and maximum (c_{max}) values of the damping coefficient is also determined by the PSO algorithm. However, the damping coefficient can take values between the defined boundaries in the skyhook control. The fraction of sprung mass acceleration which is $\frac{\dot{z}_s}{\dot{z}_s - \dot{z}_u}$ is multiplied by c_{sky} value found in Eq. (14) if the relative velocity of the sprung mass is bigger than or equal to zero. In this way, variable damping coefficient is applied to system in case of the sprung mass velocity is positive. Otherwise, the damping coefficient is equal to the minimum value (Liu, Chen, Yang, Zhang, & Yang, 2019).

The suspension control law in Eq. (15) is realized in Simulink as presented in Appendix F.

4.3 Particle Swarm Optimization (PSO)

We specify three initial minimum damping coefficients and three initial maximum damping coefficients which are within the physical damper limits determined as particles. The damper physical limits are considered to select initial particle values. After that, RMS function described in Eq. (4). is used as fitness function to compute fitness of the particles. Then, local best (p_{best}) and global best (g_{best}) positions of the particles are computed. Using a velocity formula that considers

the particle's current position, speed, and the best positions, the speed of change function is calculated as follows (Umar, 2014) (Shihabudheen, Mahesh, & Pillai, 2018):

$$v_{i+1} = w * v_i + c_1 * rand_1 * (p_{best} - x_i) + c_2 * rand_2 * (g_{best} - x_i) \quad \text{Eq. 16}$$

where w stands for the weight coefficient, v_i stands for the speed of change function, x stands for the position of the particle, c_1 and c_2 are the constants, and $rand_1$ and $rand_2$ are the random numbers (Umar, 2014) (Shihabudheen, Mahesh, & Pillai, 2018).

After movement of each particle, new positions of the particles are determined as follow Umar, 2014) (Shihabudheen, Mahesh, & Pillai, 2018):

$$x_{i+1} = x_i + v_{i+1} \quad \text{Eq. 17}$$

The fitness function is recalculated until the stopping criterion is met. In this study, stopping criterion is the number of iterations. As a result of the iteration, optimum values of minimum and maximum damping coefficients are found. The PSO algorithm is realized in MATLAB environment. In *Figure 24*, the flowchart of the PSO can be seen. The code for the PSO algorithm to determine damping parameters of both the on/off and continuous semi-active control are given in the Appendix G.

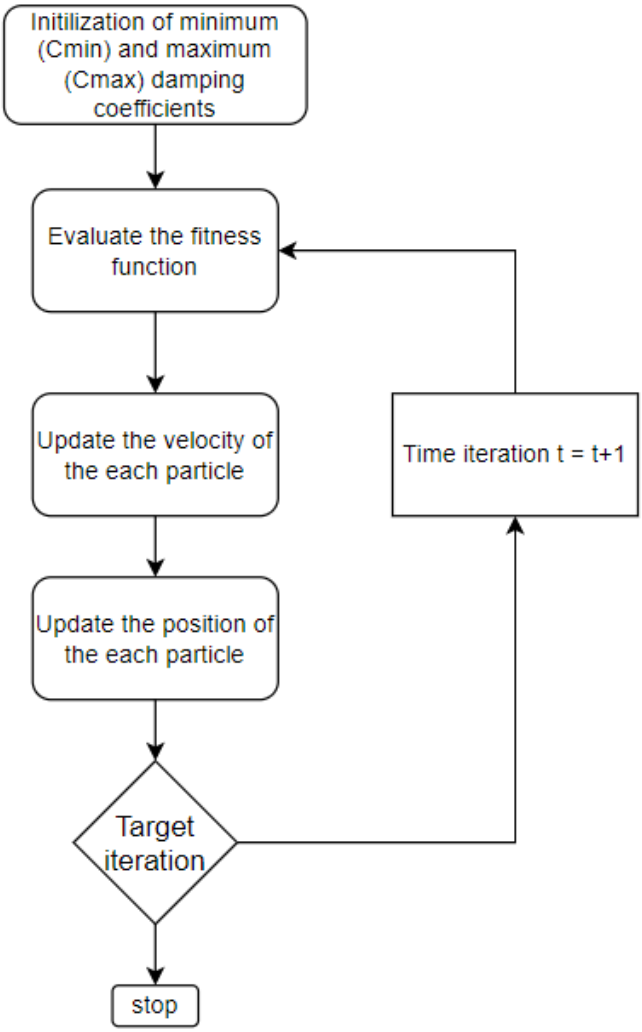

Figure 24 Flowchart of PSO.

Chapter 5

Simulation Results

The first aim of the simulations is observing steady state and transient state responses of the vehicle chassis vertical displacement and the acceleration to evaluate the performance of the passive suspension and the semi-active suspension with on-off and skyhook continuous control. We perform the simulations over the quarter car, half car and full car models (C-segment passenger car) are used for this purpose in two different scenarios: (i) driving on a standardized road profile, (ii) passing over a standard speed bumper. Also, we investigate the accuracy of the quarter car and half car models for performance evaluation via comparing the obtained results over full car model provided by AVL VSM. Moreover, the considered suspension controls are verified and evaluated through a light duty electric vehicle (VAN EV) which is widely used for carrying goods. This way, the effects of the mentioned suspension controllers on different types of vehicles are investigated.

5.1 Vehicle Parameters

To investigate the considered suspension controls' performance, we consider a compact sedan passenger car and a VAN EV of which the parameters are given in Table 1 and Table 2, respectively. The parameter values are taken from VSM environment which almost correspond to the real-life vehicles. The parameters for the half car and the quarter car models are derived from those values to obtain accurate simulation results.

Table 1

Compact Sedan (C-segment Passenger Vehicle) Parameters

Compact Sedan Vehicle Parameters	Value	Unit [SI]
Mass of chassis	1400	[kg]
Mass of front unsprung mass	35	[kg]
Mass of rear unsprung mass	40	[kg]
Front wheel track	1540	[mm]
Rear wheel track	1550	[mm]
Front wheelbase	1026	[mm]
Rear wheelbase	1674	[mm]
Chassis COG height	515.8	[mm]
Unsprung COG height	310	[mm]
Sprung mass inertia (Y)	1800	$[kgm^2]$
Suspension spring coefficient	26000	[N/m]
Suspension damper coefficient	1384.1	[N.s/m]
Tire spring coefficient	250000	[N/m]

Table 2

VAN EV (Light Duty Vehicle) Parameters

Compact Sedan Vehicle Parameters	Value	Unit [SI]
Mass of chassis	2546	[kg]
Mass of unsprung mass	45	[kg]
Front wheel track	1748	[mm]
Rear wheel track	1740	[mm]
Front wheelbase	2386.1	[mm]
Rear wheelbase	2113.9	[mm]
Chassis COG height	751.12	[mm]
Unsprung COG height	372	[mm]
Sprung mass inertia (Y)	15260	[kgm^2]
Front suspension spring coefficient	63000	[N/m]
Rear suspension spring coefficient	70000	[N/m]
Front suspension damper coefficient	3081.2	[N.s/m]
Rear suspension damper coefficient	5432.6	[N.s/m]
Tire spring Coefficient	307300	[N/m]

5.2 Road Profiles

The effects of suspension control systems on the vehicle are examined in time domain. The simulations are performed by considering two different road scenarios which are ISO8608 (Class B, V=25kph) random disturbance profile and trapezoidal speed bump with 0.1-meter height.

5.2.1 ISO 8608 road profile. In general, vehicles are exposed to a random road profile rather than a determined road profile to investigate the vertical dynamic behaviour of the vehicle in real-life conditions. For this purpose, ISO 8608 standard proposes a road disturbance classification methodology by using a power spectral density (PSD) function described as

$$\Phi(\Omega) = \Phi(\Omega_0)\left(\frac{\Omega}{\Omega_0}\right)^{-\omega} \quad \text{Eq. 18}$$

where

Ω: angular spatial frequency in rad/m,

Ω_0: reference angular spatial frequency which is 1 rad/m,

ω: exponent of fitted PSD (it is taken as 2 if constant velocity is applied.),

$\Phi(\Omega_0)$: PSD value according to reference angular spatial frequency.

ISO 8608 standard define A to H road profile as a disturbance in frequency domain with PSD function Eq. (18). According to the PSD values given in Table 3, a random road profile is generated. Class B according to ISO 8608 is used to analyse the implemented suspension control behaviour in this thesis (Salmani, Abbasi, Fahimi Zand, Fard, & Nakhaie Jazar, 2022) (Kırbaş & Karaşahin, 2023) (Goenaga, Fuentes, & Mora, 2017)

Table 3

ISO 8608 Road Classification

Road Class	Value $\Phi(\Omega_0)\frac{10^{-6}m^2}{rad/m}$
A (very good)	4
B (good)	16
C (average)	64
D (poor)	256
E (very poor)	1024
F	4096
G	16384
H	65536

It is feasible to create an artificial road profile using the expression if the PSD function of vertical displacements is known, as demonstrated by several authors (Rossi & Lucente, 2004) which is expressed mathematically as follows (ISO 2631-1:1997, 1997).

$$h(x) = \sum_{i=0}^{n} \sqrt{(\Delta n)}\ 2^k 10^{-3} (\frac{n_0}{i.\Delta n}) \cos\ (2\pi i \Delta n x + \varphi) \qquad \text{Eq. 19}$$

where

φ: random phase angle [0 2π],

x: longitudinal variable in x- direction [0 L],

n: spatial frequency in cycles/m,

n_0: reference spatial frequency which is 0.1 rad/m,

Δn: 1/n,

and *k* values are described in Table 4.

Table 4

Vertical Displacement of Road Profile

Upper Limit	Lower Limit	k value
A	B	3
B	C	4
C	D	5
D	E	6
E	F	7
F	G	8
G	H	9

MATLAB software coding enables the realization of random road input generation based on the above mathematical expressions and procedures. According to the Class B Road profile and the vehicle velocity 25kph, the random road disturbance graph in time domain can be obtained as shown in *Figure 25*.

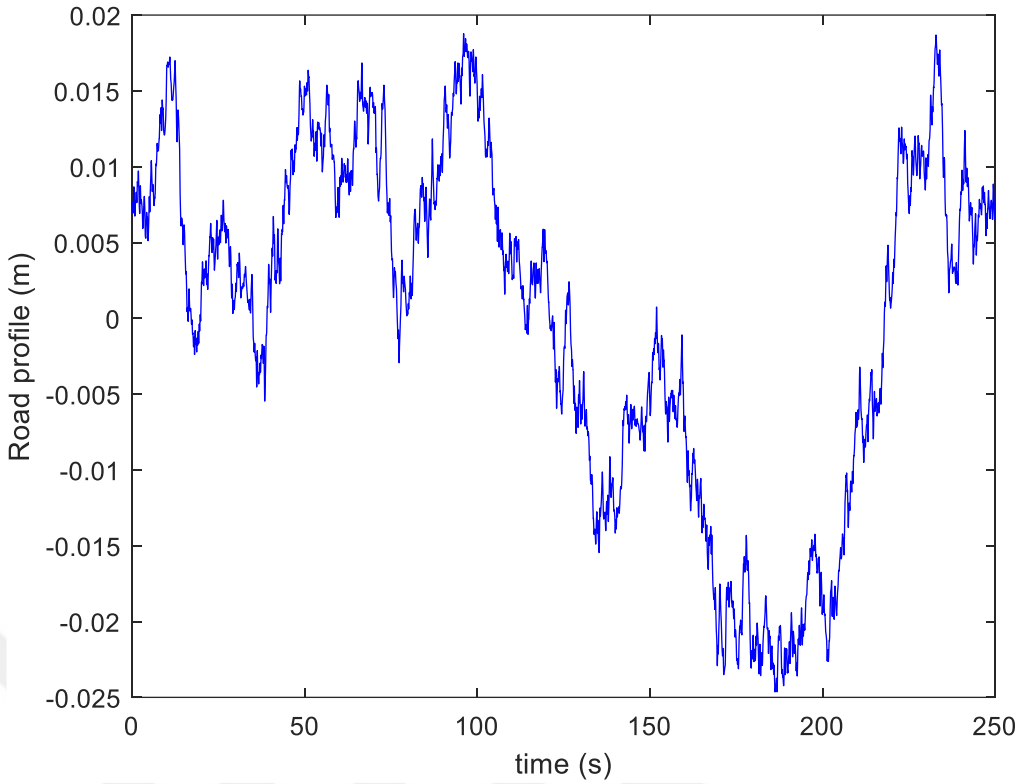

Figure 25 ISO 8608 road profile (V=25kph) B-class road

5.2.2 Trapezoidal speed bump. There is a regulation which come into force on 28th April 1999 and called "The Highways (Road Humbs)" describing the dimensional standards of the speed bumper (The Secretary of State for the Environment, Transport and the Regions, 1999). The speed bumps may cause hazardous events which vehicle encounter if dimensions and location of them are not regulated. Therefore, standardized bumper is used in this thesis to see real behaviour of the suspension. According to the mentioned regulation, the requirements of the proper speed bump is given in Table 5.

The speed bumps are located on the roads where the speed limit is lower than 30mph. We consider the vehicle with fixed speed at 18kph passing a speed bumper with the specifications in Table 5 which corresponds to a change in road height versus time as illustrated in *Figure 26*. The given signal is used in simulations as a speed bumper to evaluate the suspension control performance.

Table 5

Speed Bumper Regulation Parameters

Dimension Parameters	Value	Unit [SI]
Length in minimum	900	$[mm]$
Height in minimum	25	$[mm]$
Height in maximum	100	$[mm]$
Gradient in maximum	1:10	$[mm]$

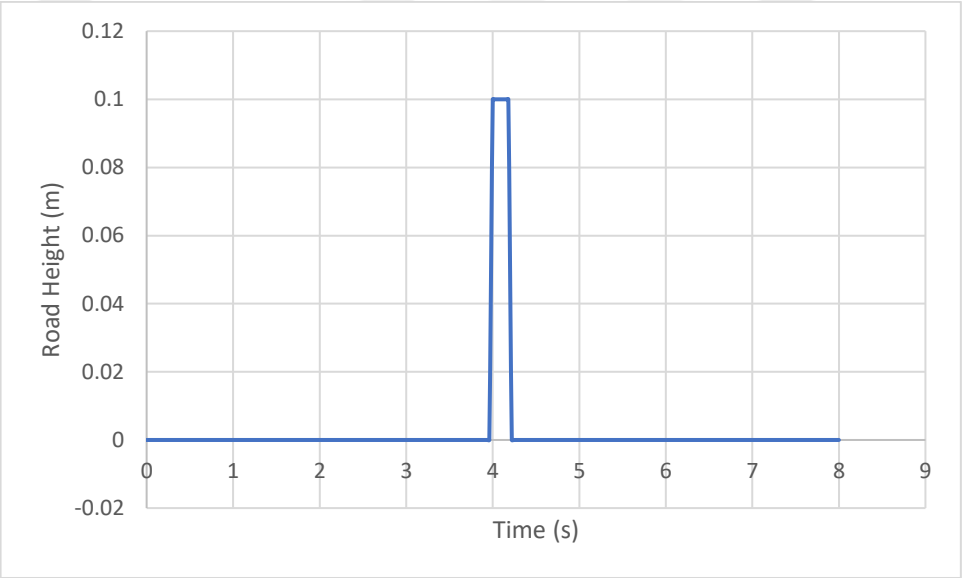

Figure 26 Speed bumper based on "Highways England, and Wales the Highways (Road Humps) Regulations 1999 (25kph)"

5.3 Evaluation of Suspension Systems for a Compact Sedan Car

A conventional C-segment passenger vehicle is investigated for performance evaluation of the passive suspension, the semi-active on-off and the skyhook continuous controlled suspension. PSO is used to minimize the RMS sprung mass acceleration in Eq. (4) to determine the minimum and maximum values of damping coefficients for the considered semi-active on/off and continuous suspension controls as described in Section 4.2 over the simulation data obtained from the quarter car and

half car models provided in Section 3.1. and 3.2, respectively. The suspension parameters are determined via optimization for two different road scenarios. In the first one, the vehicle is crossing over a trapezoidal speed bumper described in Section 4.2.2. In the second scenario, the vehicle is moving on the ISO 8608 Class B Road profile with a fixed speed of 25 kph. The PSO algorithm is employed over the simulation data for these two scenarios. Then, the suspension control with the optimized parameters over two different vehicle models are compared in terms of consistency to each other. Finally, optimized parameters over quarter car model are applied to VSM full car vehicle simulation model to see the real dynamic behaviour of the vehicle.

5.3.1 Evaluation of suspension systems over quarter car model. Ride comfort highly depends on first overshoot of sprung mass. Two quarter car models are derived from the vehicle parameters given in Table 1 to represent front and rear quarter portions of the vehicle separately. The reason of separate optimization is the difference of the unsprung masses for front and rear axles, namely 35 kg for the front suspension and 40 kg for the rear suspension. For the speed bump passing scenario, the vertical accelerations of the passenger car by considering front quarter portion are plotted in Figure 27 when the passive, semi-active on/off and skyhook-controlled suspensions are applied where the semi-active suspension control parameters are determined via PSO as given in Table 6 with optimal RMS of vertical acceleration values. The optimized suspension control parameters and corresponding RMS values for the rear axles are also given in Table 7. It is clearly seen from both Table 6, Table 7 and Figure 27 that the continuous skyhook-controlled suspension damping performance is the best over passive and semi-active on/off suspensions.

Table 6

RMS of Vertical Acceleration and Optimized Parameters for Suspension Control over Quarter Car of Compact Sedan Passing over Speed Bump by Considering Front Left Quarter Vehicle Model

Suspension System	***RMS of Ver. Acc.*** *[m/s²]*	***Improvement (%)***	c_{min} [N.s/m]	c_{max} [N.s/m]
No Control (Passive)	1.3361	-	1384.07	1384.07
Semi-active on/off	1.1246	15.83	766.67	1552.30
Skyhook Continuous	1.0452	21.77	766.67	3000.00

Table 7

RMS of Vertical Acceleration and Optimized Parameters for Suspension Control over Quarter Car of Compact Sedan Passing over Speed Bump by Considering Rear Left Vehicle Model

Suspension System	***RMS of Ver. Acc.*** *[m/s²]*	***Improvement (%)***	c_{min} [N.s/m]	c_{max} [N.s/m]
No Control (Passive)	2.1042	-	1384.07	1384.07
Semi-active on/off	1.7531	16.69	768.02	1738.40
Skyhook Continuous	1.6704	20.62	766.67	3000.00

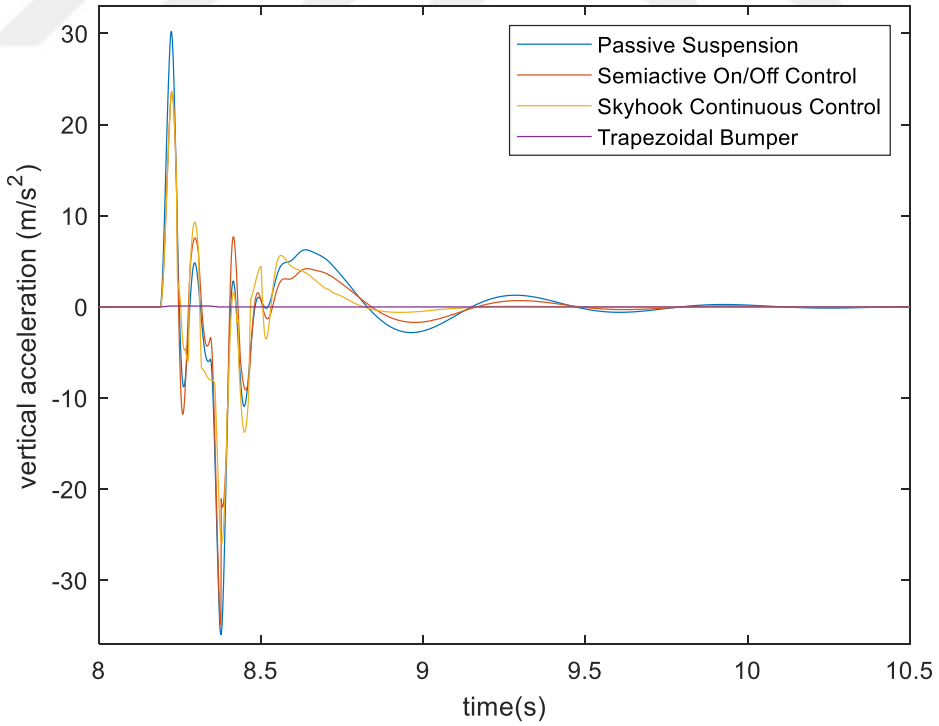

Figure 27 Quarter-car (front left) vertical acceleration performance comparison among the considered suspensions for the Compact Sedan over a speed bump

On the other hand, the semi-active on/off system's vertical displacement behaviour is better than the skyhook-controlled suspension as seen in *Figure 28*. The reason behind this difference between acceleration and displacement behaviour is due to the use of RMS vertical acceleration as a cost function in PSO algorithm to determine the optimal suspension damping ratio limits. This cost function is preferred because the vehicle ride comfort is more related to the vertical chassis acceleration. For that reason, we state that the skyhook-controlled suspension provides the best performance in terms of ride comfort over a speed bump.

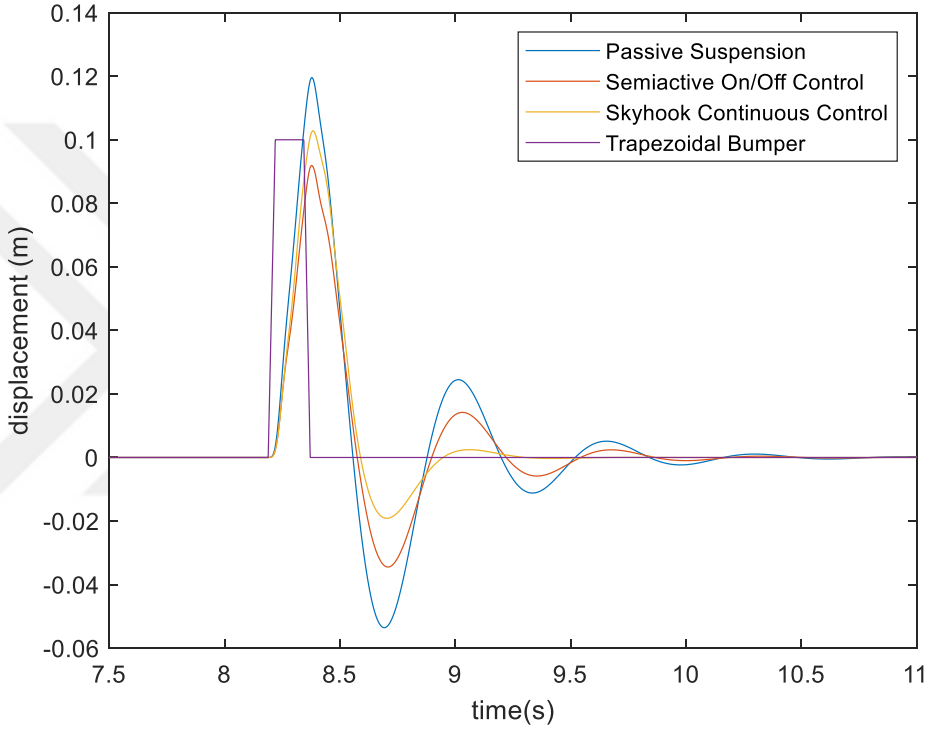

Figure 28 Quarter-car (front left) vertical displacement performance comparison among the considered suspensions for the Compact Sedan over a speed bump

We also optimize the semi-active suspension damping parameters via PSO over the data from the vehicle simulation model driven on ISO 8608 road profile. The optimum RMS of vertical accelerations of the vehicle and the suspension parameters are found as in Table 8 and Table 9. The time history of the chassis vertical acceleration is plotted in *Figure 29*. As seen from Table 8 and Table 9, we conclude that the skyhook continuous suspension control achieves better performance as compared to the other considered suspension systems.

Table 8

RMS of Vertical Acceleration and Optimized Parameters for Suspension Control over Quarter Car of Compact Sedan Passing over ISO 8608 Road Profile by Considering Front Left Quarter Vehicle Model

Suspension System	***RMS of Ver. Acc.*** *[m/s²]*	***Improvement (%)***	c_{min} [N.s/m]	c_{max} [N.s/m]
No Control (Passive)	0.2714	-	1384.07	1384.07
Semi-active on/off	0.2400	11.57	766.67	1488.60
Skyhook Continuous	0.2230	17.83	766.67	3000.00

Table 9

RMS of Vertical Acceleration and Optimized Parameters for Suspension Control over Quarter Car of Compact Sedan Passing over ISO 8608 Road Profile by Considering Rear Left Quarter Vehicle Model

Suspension System	***RMS of Ver. Acc.*** *[m/s²]*	***Improvement (%)***	c_{min} [N.s/m]	c_{max} [N.s/m]
No Control (Passive)	0.4106	-	1384.07	1384.07
Semi-active on/off	0.3645	11.23	767.45	1391.70
Skyhook Continuous	0.3393	17.36	766.67	3000.00

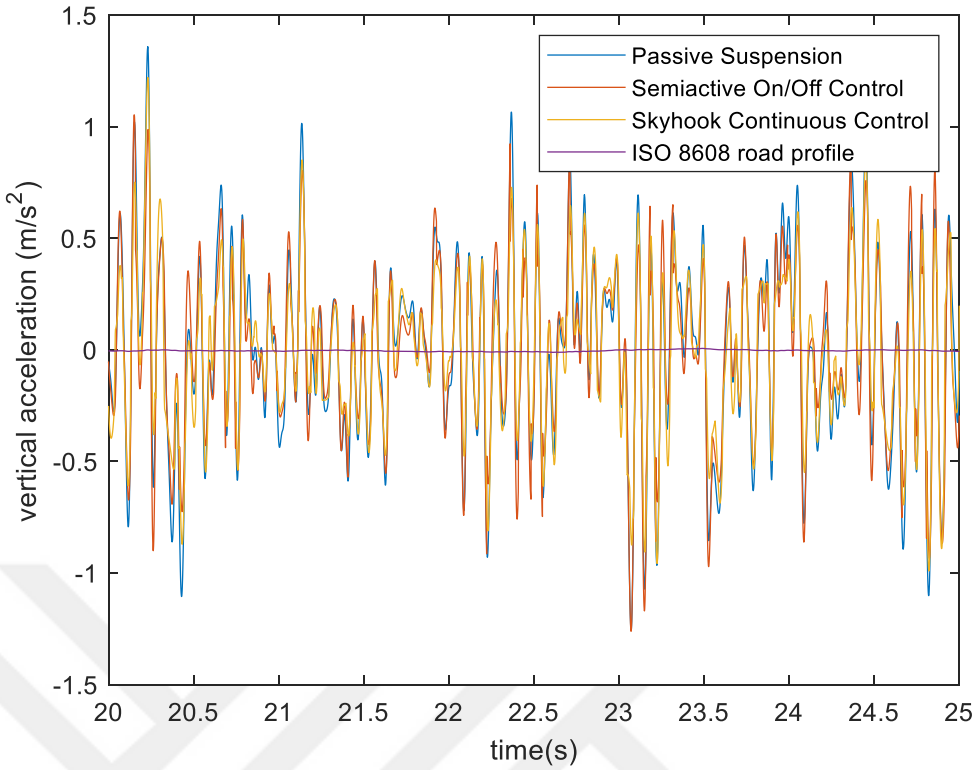

Figure 29 Quarter-car (front left) vertical acceleration performance comparison among the considered suspensions for the Compact Sedan over a ISO8608 road profile

The vertical displacement of the chassis versus time is illustrated in *Figure 30*. Similar to the speed bumper scenario, the semi-active on/off suspension control performs the best in the sense of least vertical displacements.

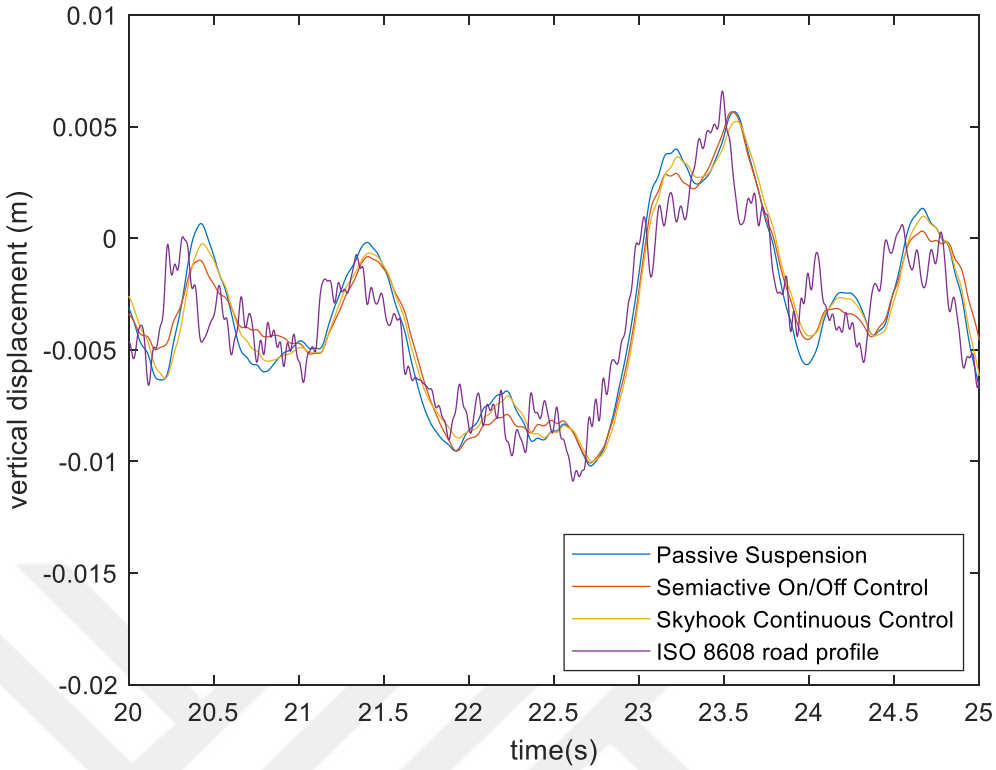

Figure 30 Quarter-car (front left) vertical displacement performance comparison among the considered suspensions for the Compact Sedan over a ISO8608 road profile

5.3.2 Evaluation of suspension systems over half car model. In this subsection, the bicycle half car model is used to obtain simulation results where the suspension control with the damping parameters found by PSO algorithm over the half car model simulation data. PSO is modified for half car model. Firstly, the rear damping coefficients are kept constant and the front damping coefficients are optimized. Then, the optimized front damping coefficients are applied to the vehicle and the rear damping coefficients are optimized. The objective is to see the effects of the two different vehicle dynamic models on determination of the damping coefficient limits. The only significant difference between quarter and half car models which affect the PSO damping coefficients and simulation results is inertial moment of chassis while crossing the speed bump and driving on the ISO 8608 road profile. This effect causes slight decrements on RMS improvement values in suspension control performance results in speed bump passing scenario when it is compared with the quarter car model suspension behaviour as seen in Table 6, Table 7, Table 10 and Table 11.

Table 10

Front Left *RMS of Vertical Acceleration and Optimized Parameters for Suspension Control over Half Car of Compact Sedan Passing over Speed Bump*

Suspension System	***RMS of Ver. Acc.*** *[m/s²]*	***Improvement (%)***	c_{min} [N.s/m]	c_{max} [N.s/m]
No Control (Passive)	0.8781	-	1384.07	1384.07
Semi-active on/off	0.7649	12.89	781.19	1397.30
Skyhook Continuous	0.7221	17.77	783.48	1385.10

Table 11

Rear Left *RMS of Vertical Acceleration and Optimized Parameters for Suspension Control Over Half Car of Compact Sedan Passing over Speed Bump*

Suspension System	***RMS of Ver. Acc.*** *[m/s²]*	***Improvement (%)***	c_{min} [N.s/m]	c_{max} [N.s/m]
No Control (Passive)	0.8781	-	1384.07	1384.07
Semi-active on/off	0.7685	12.48	1205.6	1386.30
Skyhook Continuous	0.7237	17.58	1351.5	1410.40

Moreover, RMS improvement values are almost the same in suspension control performance results in ISO8608 when it is compared with the quarter car model

suspension behaviour as seen in Table 8, Table 9, Table 12 and Table 13. The reason behind is that both the front and rear suspensions behave almost the same over the road disturbances due to identical damper limits for the compact class vehicle. The only difference which affects the RMS is moment of inertia due to wheelbase and the relevant mass distribution of the chassis. However, these effects can be neglected to simplify suspension design for identical suspension damping coefficient vehicles.

Table 12

Front Left *RMS of Vertical Acceleration and Optimized Parameters for Suspension Control over Half Car of Compact Sedan Passing over ISO 8608 Road Profile*

Suspension System	***RMS of Ver. Acc.*** *[m/s²]*	***Improvement (%)***	c_{min} [N.s/m]	c_{max} [N.s/m]
No Control (Passive)	0.1732	-	1384.07	1384.07
Semi-active on/off	0.1565	9.64	781.96	1384.20
Skyhook Continuous	0.1424	17.78	768.52	1395.70

Table 13

Rear Left *RMS of Vertical Acceleration and Optimized Parameters for Suspension Control over Half Car of Compact Sedan Passing over ISO 8608 Road Profile*

Suspension System	***RMS of Ver. Acc.*** *[m/s²]*	***Improvement (%)***	c_{min} [N.s/m]	c_{max} [N.s/m]
No Control (Passive)	0.1732	-	1384.07	1384.07
Semi-active on/off	0.1567	9.53	1383.20	1453.10
Skyhook Continuous	0.1424	17.78	1375.00	1399.30

Time histories in *Figure 31* and *Figure 32* where the vertical accelerations and displacements for each suspension control system are depicted, respectively over speed bumper. For the ISO 8608 road profile scenario, the time histories of the vertical acceleration and displacement are also demonstrated in *Figure 33* and *Figure 34*, respectively. From the respective figures and tables, we state that the results are in parallel with the quarter car vehicle models.

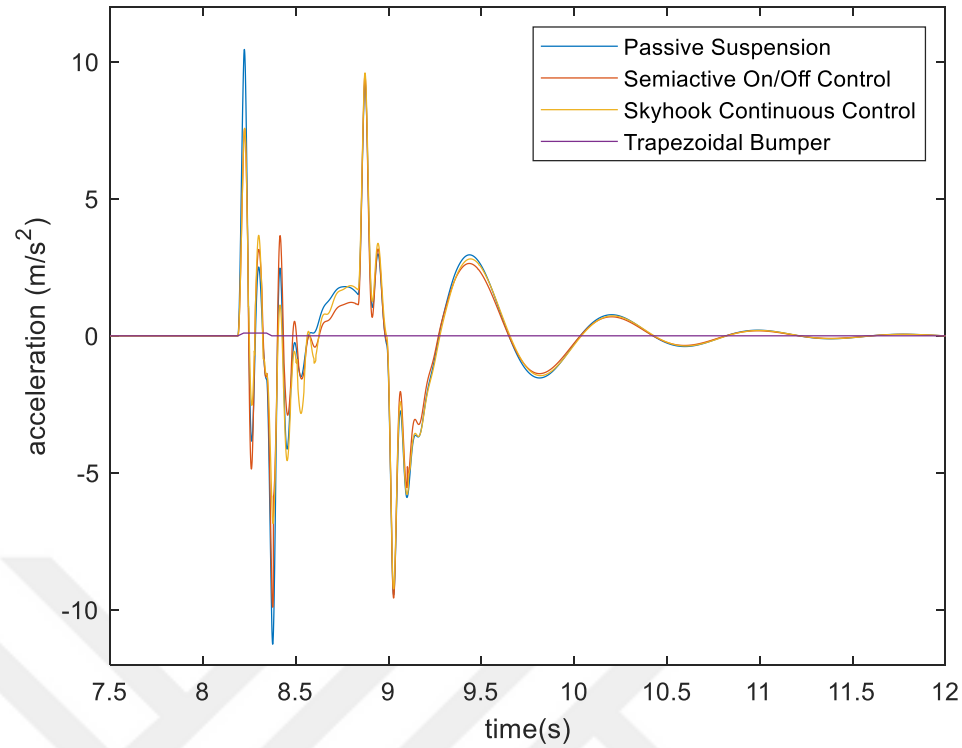

Figure 31 Half-car vertical acceleration performance comparison among the considered suspensions for the Compact Sedan over a speed bump.

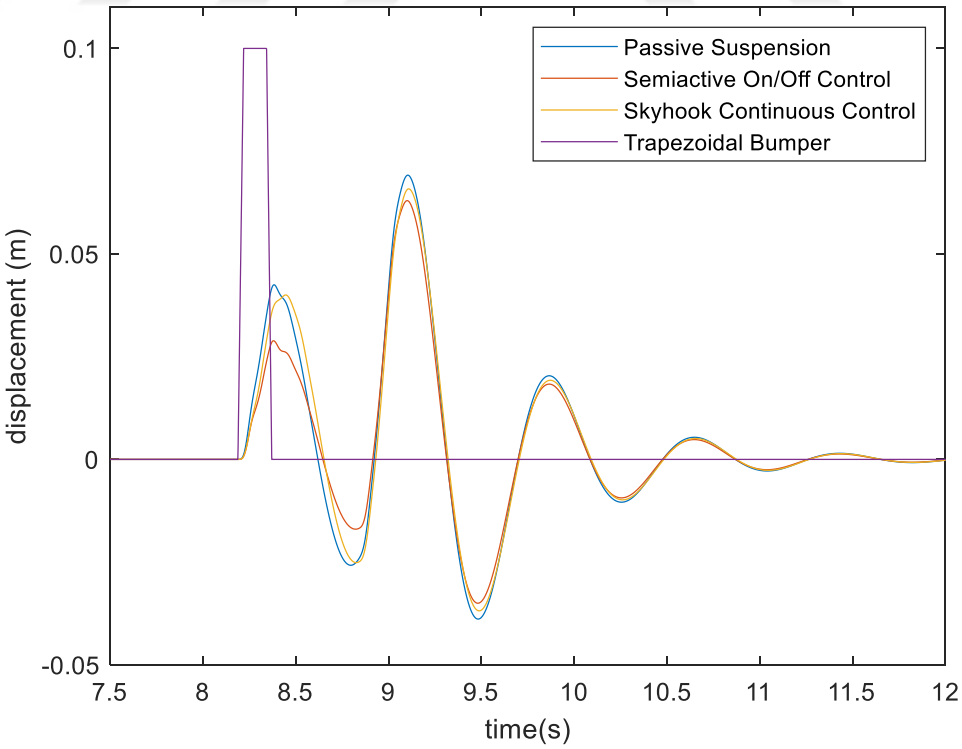

Figure 32 Half-car vertical displacement performance comparison among the considered suspensions for the Compact Sedan over a speed bump.

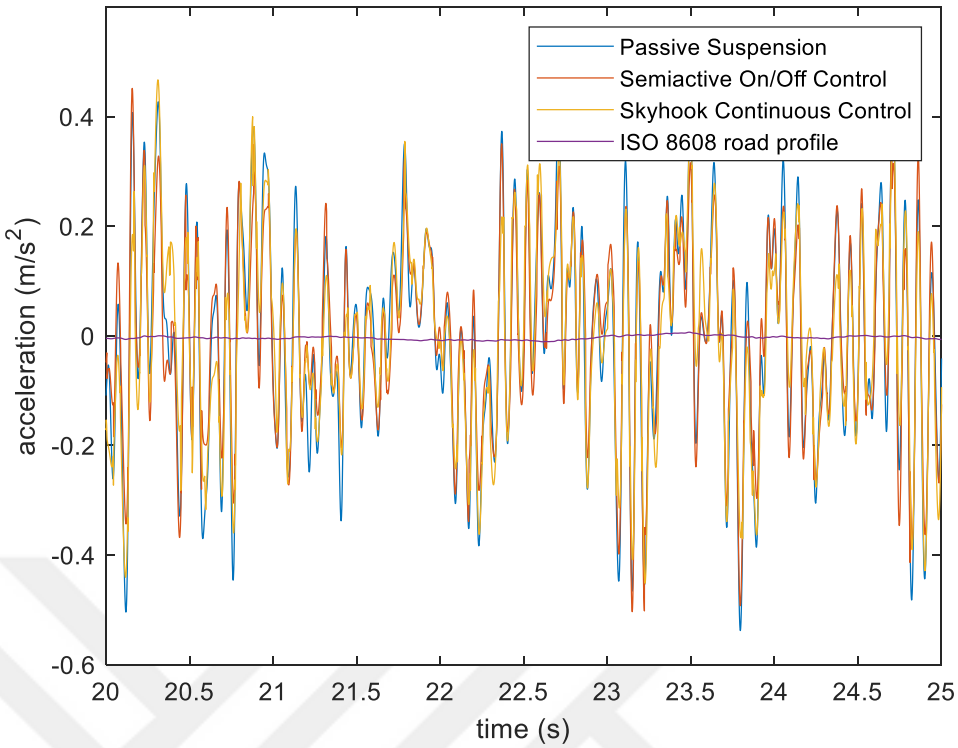

Figure 33 Half-car vertical acceleration performance comparison among the considered suspensions for the Compact Sedan over a ISO8608 road profile.

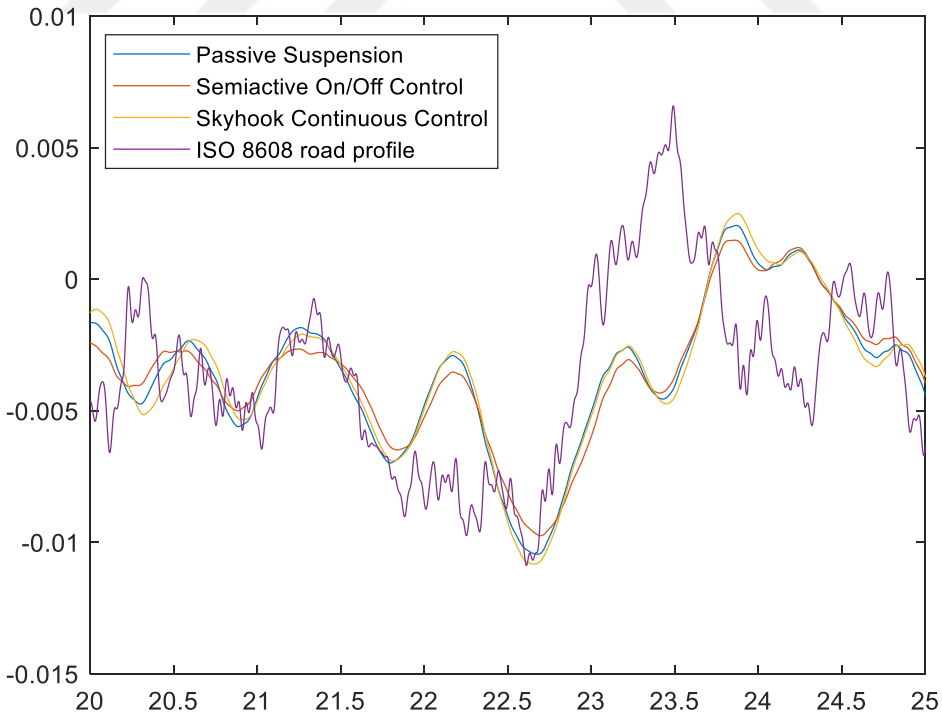

Figure 34 Half-car vertical displacement performance comparison among the considered suspensions for the Compact Sedan over a ISO8608 road profile.

5.3.3 Evaluation of suspension systems over VSM full car model. Unlike the car models created in Simulink environment, the VSM full car model is a non-linear one which contains all the components of a real vehicle. Therefore, the effects of other component interactions such as mechanical torsions, stresses among linkages and the other various vehicle dynamics are not neglected in VSM environment. To see the real dynamic behaviour of the vehicle we prefer to keep the nonlinear rigid body dynamics of the full-car model as well as the nonlinearities in static camber, and in mechanical trail which have direct effects on vertical behaviour of the vehicle. Moreover, loaded (when the passengers exist) tyre radius and transient tyre parameters which are directly related to vertical behaviour of the chassis are also kept.

According to the optimized RMS of vertical acceleration given in Table 14, both semi active on/off and skyhook continuous controlled suspension gives good ride comfort for both road scenarios. For the speed bumper scenario, the time histories of the vertical acceleration and displacement are demonstrated in *Figure 35* and *Figure 36*, respectively.

For the ISO 8608 road profile scenario, the time histories of the vertical acceleration and displacement are also demonstrated in *Figure 37* and *Figure 38*, respectively. From the respective figures and tables, we state that controlled suspensions are able to enhance vehicle ride comfort as quarter and half car models implies. Moreover, it is seen that the continuous skyhook-control law provides overshoot, i.e. peak values, less than the on/off control law in contrast to the simulations performed through simplified linear models.

Table 14

RMS of Vertical Acceleration for Suspension Control of Compact Sedan Passing over Speed Bumper and ISO 8608 Road Profile for AVL VSM Model

Suspension System	***RMS of ISO 8608 Ver. Acc.*** *[m/s²]*	***Improvement on ISO 8608***	***RMS of Speed Bumper Ver. Acc.*** *[m/s²]*	***Improvement on Speed Bump***
No Control (Passive)	0.4910	-	1.9310	-
Semi-active on/off	0.4791	2.42	1.8406	4.68
Skyhook Continuous	0.4374	10.91	1.6404	15.05

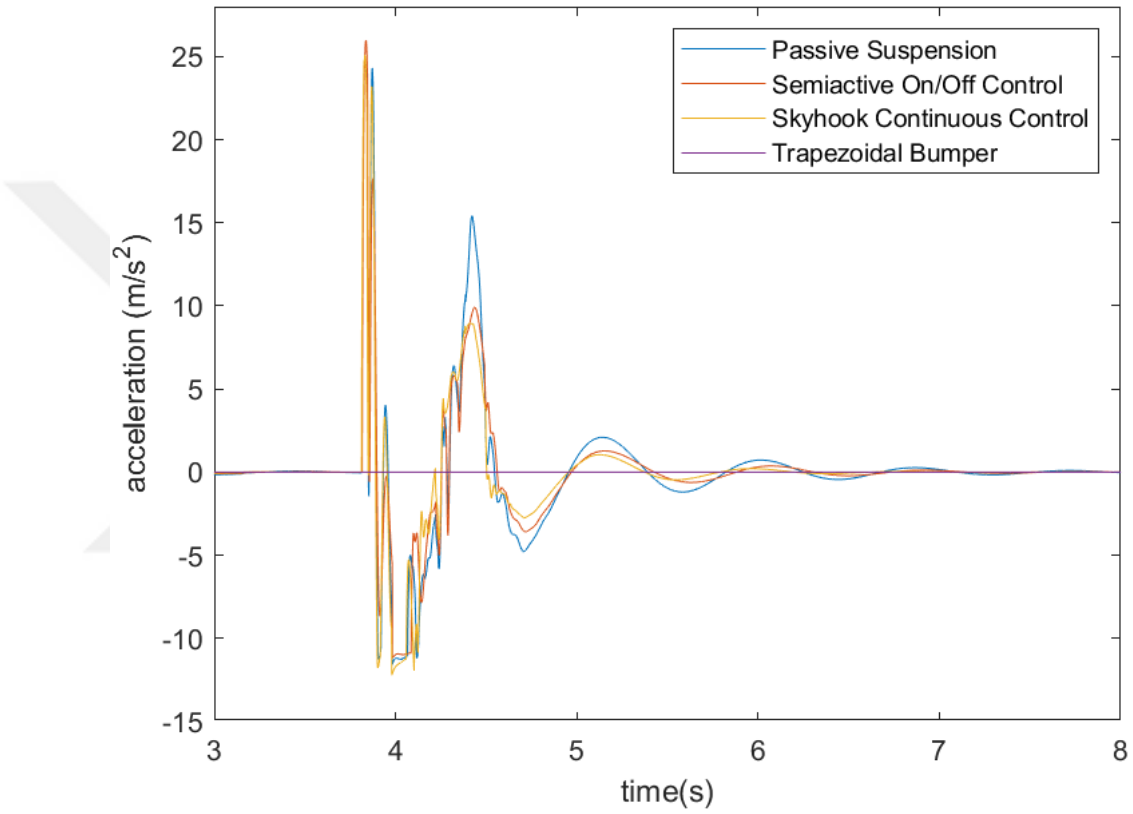

Figure 35 VSM Full-car vertical acceleration performance comparison among the considered suspensions for the Compact Sedan over a speed bump.

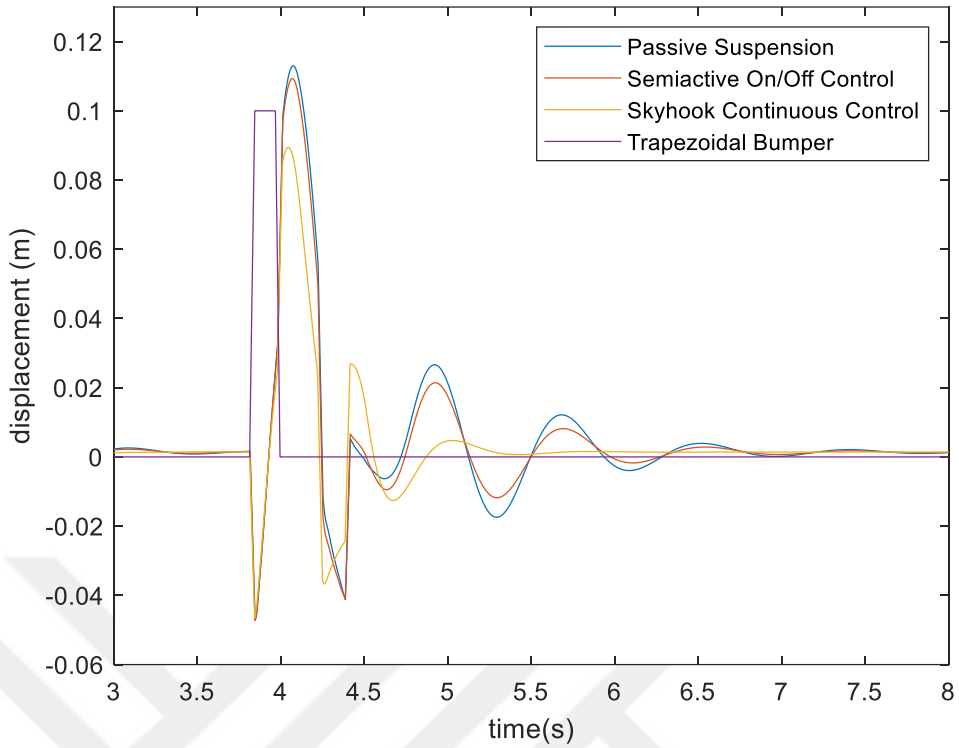

Figure 36 VSM Full-car vertical displacement performance comparison among the considered suspensions for the Compact Sedan over a speed bump.

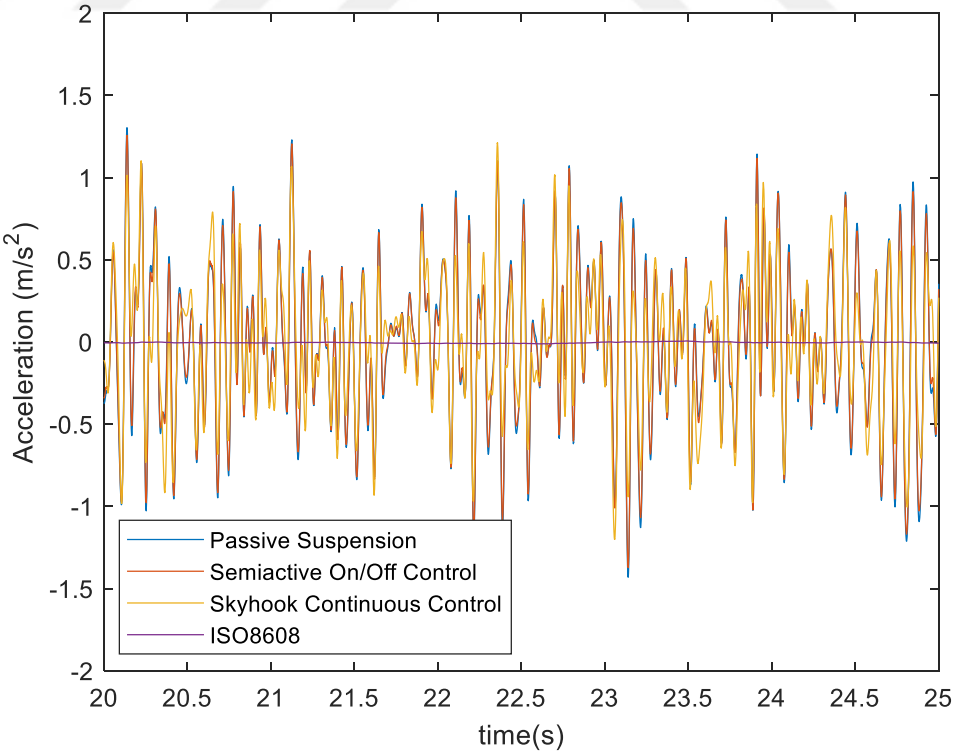

Figure 37 VSM Full-car vertical acceleration performance comparison among the considered suspensions for the Compact Sedan over a ISO8608 road profile.

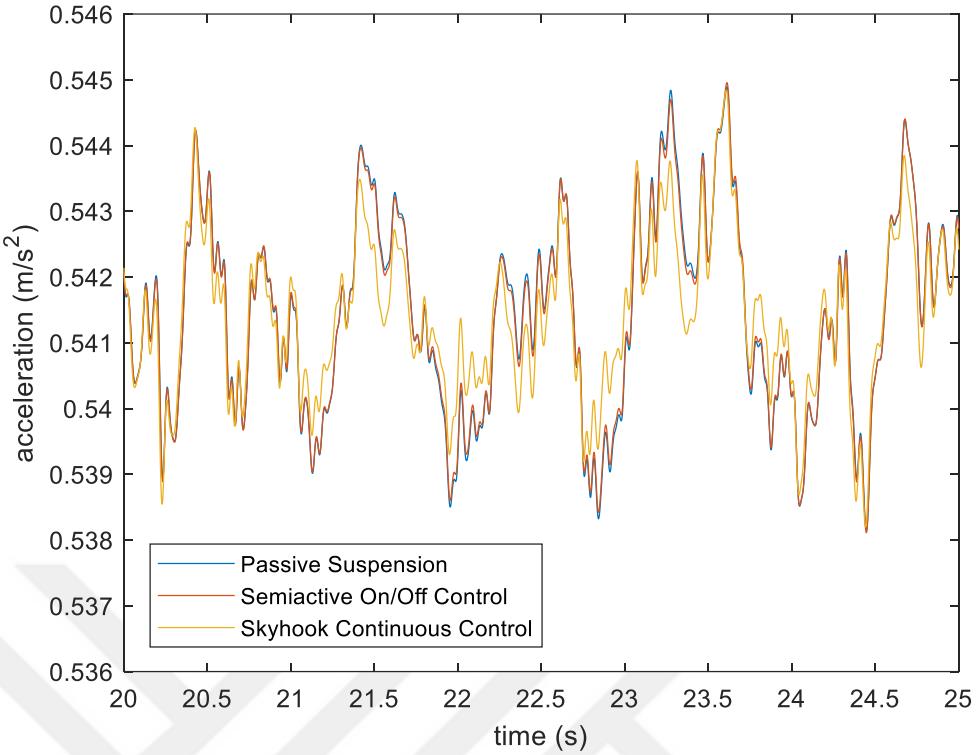

Figure 38 VSM Full-car vertical displacement performance comparison among the considered suspensions for the Compact Sedan over a ISO8608 road profile.

5.4 Comparison of Suspension Control Systems Over All Models for Compact Sedan

The simulation results for the half car model with passive, semi-active on/off and skyhook continuous suspensions are coherent with the VSM full car model for the considered compact Sedan passenger car. This result is expected because the vehicle is driven through straight road with constant speed. In fact, it does not expose to yaw moment of inertia over both speed bumper and ISO 8608 road profile. Therefore, half car dynamic model is adequate to simulate the vertical dynamic behaviour of the vehicle, so that this model match well with VSM full car model for all suspension types. On the other hand, the simulations over the quarter car model does not fit well to the half car and VSM full car vehicle models because pitch moment of inertial effects cannot be simulated via simplified quarter car model. In fact, we observe much higher amplitude in VSM model when compared with the other simplified linear models due to the rise of nonlinear dynamics of several real vehicle components. To

see the mentioned coherence and deviation among the models, one can check the Figure 39-44 which provide the time histories of the vertical acceleration and the displacement with the considered suspension controls for both road scenarios.

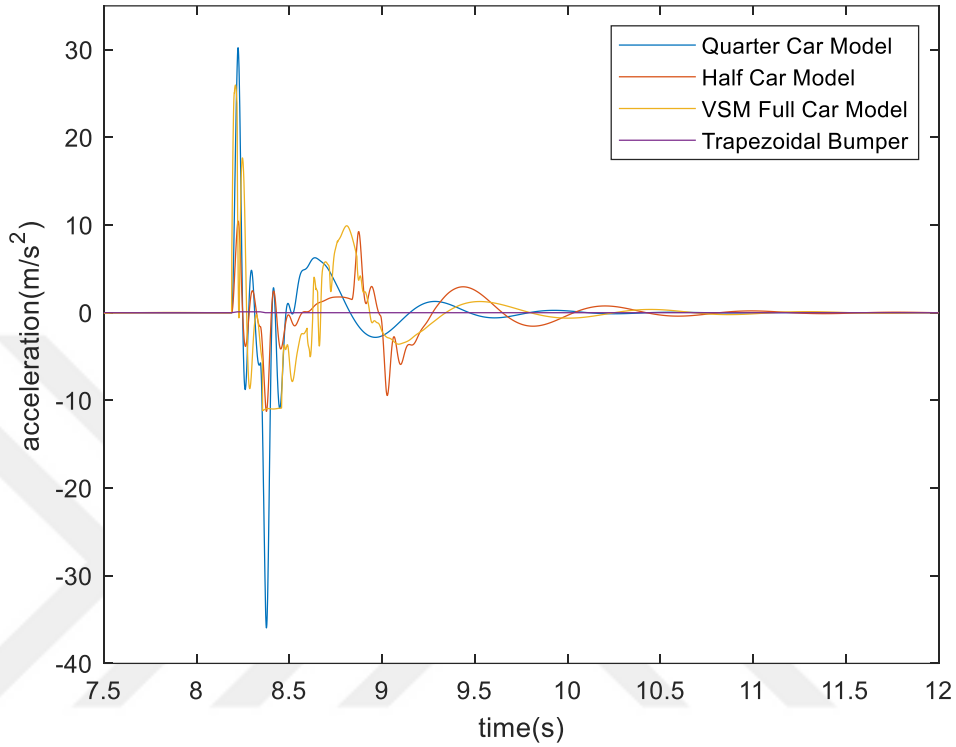

Figure 39 Passive suspension accuracy evaluation for quarter, half and VSM full car vehicle models over a speed bump.

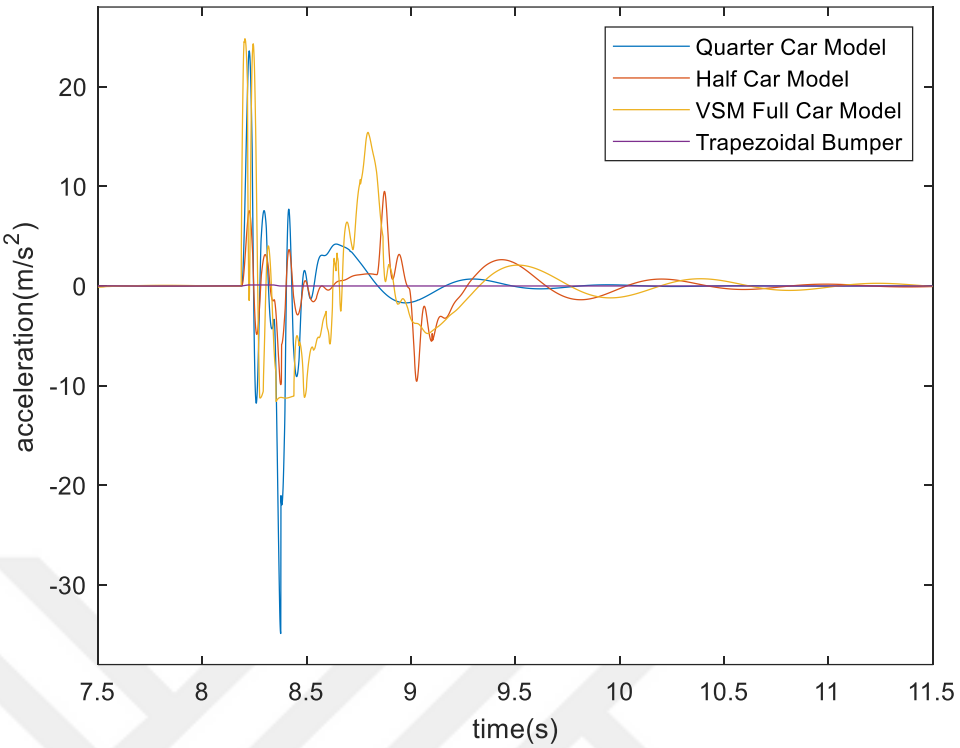

Figure 40 Semi-active on/off suspension accuracy evaluation for quarter, half and VSM full var vehicle models over a speed bump.

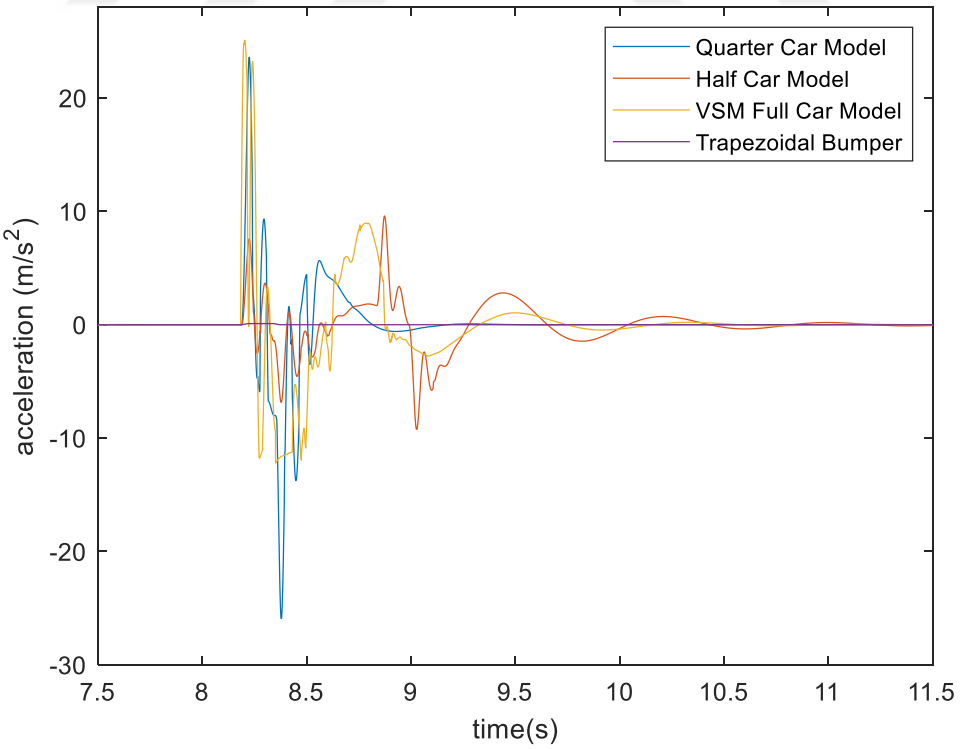

Figure 41 Skyhook continuous suspension accuracy evaluation for quarter, half and VSM full var vehicle models over a speed bump

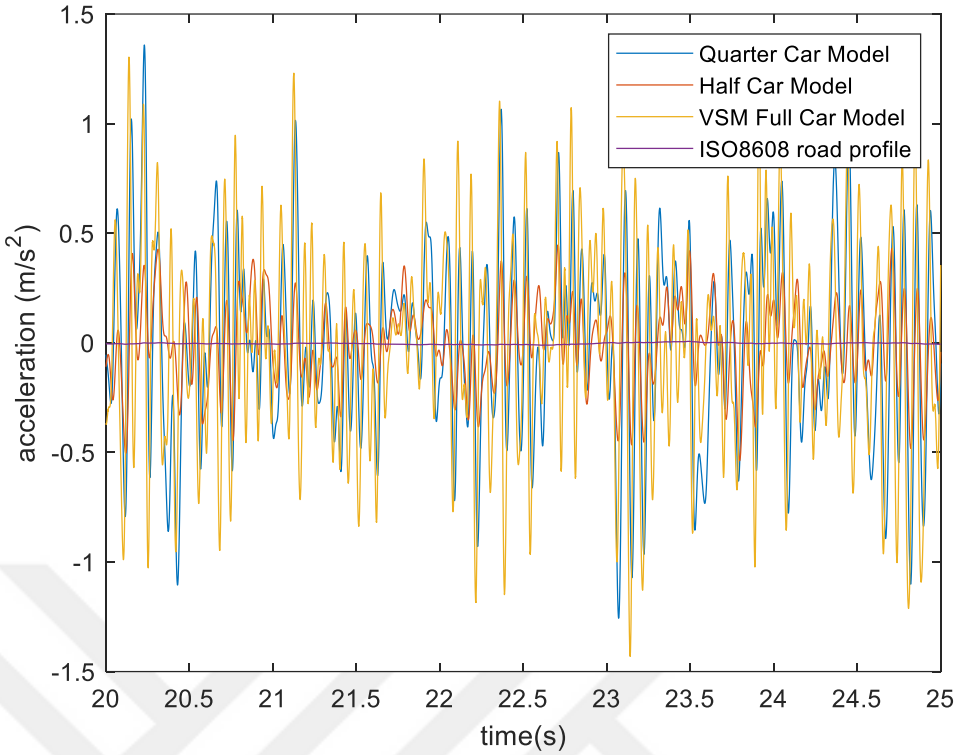

Figure 42 Passive suspension accuracy evaluation for quarter, half and VSM full var vehicle models over ISO8608 road input.

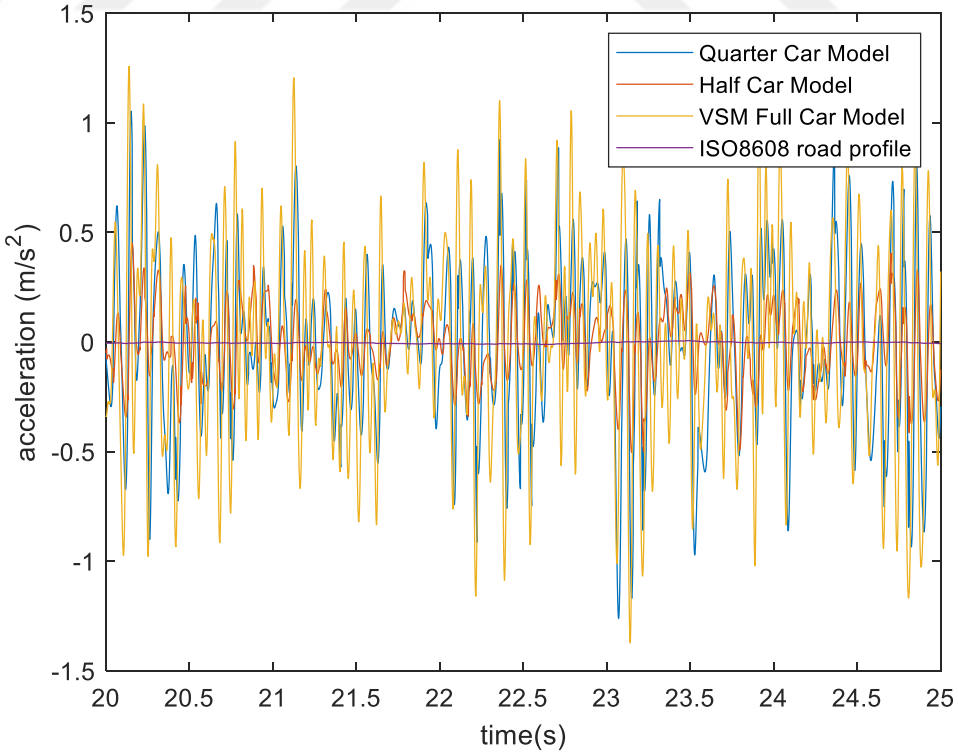

Figure 43 Semi-active on/off suspension accuracy evaluation for quarter, half and VSM full var vehicle models over ISO8608 road input.

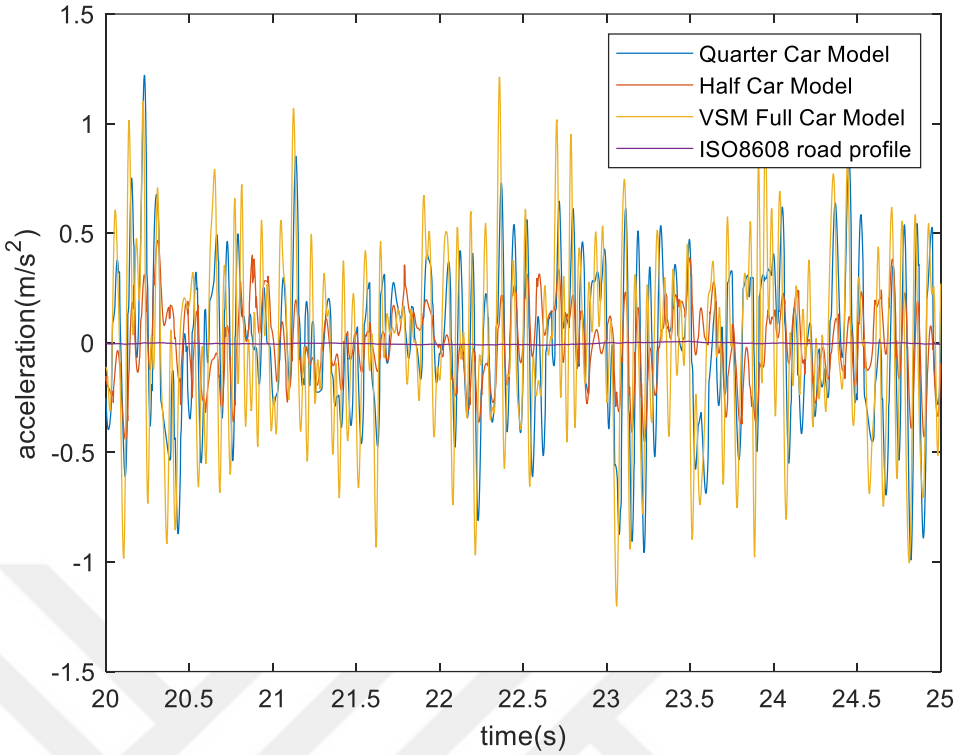

Figure 44 Skyhook continuous control suspension accuracy evaluation for quarter, half and VSM full var vehicle models over a ISO8608 road profile.

5.5 Evaluation of Suspension Systems For VAN EV Light Duty Vehicle

Commercial (VAN EV light duty) vehicle suspension parameters differ from compact class (C-segment passenger) vehicles. This is because the suspensions in line with front axes and suspensions in line with rear axles have different spring coefficients as well as different damping ratios. Therefore, the utilized PSO algorithm is modified to handle this difference. PSO optimizes the minimum and the maximum values of damping ratios (both front and rear separately) according to the front left RMS vertical acceleration value over the half-car vehicle model. By means of the considered half car vehicle model, it is possible to observe the front and rear axles dynamic behaviour in terms of vertical displacement and acceleration. Thus, the half car vehicle model is chosen to implement PSO algorithm to optimize the front and rear damping coefficients in semi-active suspension controls. The code for PSO given in Appendix G is slightly modified as follows. Firstly, the rear side of the damping ratio is chosen to be passive value and accordingly optimization is done on front suspension

based on both semi-active on/off and skyhook continuous controls through simulation. Secondly, the front side of the damping ratio is chosen to be previously optimized values and the same process is duplicated. Optimization is conducted based on the RMS value of front left vertical acceleration of half car vehicle model. The speed bumper and ISO 8608 road profile scenarios are used to perform simulation based PSO algorithm. The optimized RMS of vertical acceleration and the corresponding damping coefficient limits in semi-active suspension control laws in Eqs. (4) and (15) are given for both road scenarios in Table 16, Table 17, Table 18, and Table 19.

Table 15

RMS of Vertical Acceleration and Optimized Parameters for Suspension Control over Half Car Model of VAN EV Passing over Speed Bump for Front Axle

Suspension System	***RMS of Ver. Acc.*** *[m/s²]*	***Improvement (%)***	$c_{\min,front}$ [N.s/m]	$c_{max,front}$ [N.s/m]
No Control (Passive)	1.2793	-	3081.16	3081.16
Semi-active on/off	1.1356	11.23	1029.20	5175.50
Skyhook Continuous	1.1119	13.08	1028.60	4774.20

Table 16

RMS of Vertical Acceleration and Optimized Parameters for Suspension Control over Half Car Model of VAN EV Passing Over Speed Bump for Rear Axle

Suspension System	***RMS of Ver. Acc.*** *[m/s²]*	***Improvement (%)***	$c_{min,rear}$ [N.s/m]	$c_{max,rear}$ [N.s/m]
No Control (Passive)	1.2793	-	5432.64	5432.64
Semi-active on/off	1.1300	11.67	5427.00	11643.00
Skyhook Continuous	1.1152	12.83	5413.80	11597.00

Table 17

RMS of Vertical Acceleration and Optimized Parameters for Suspension Control over Half Car Model of VAN EV Passing over ISO 8608 Road Profile for Front Axle

Suspension System	***RMS of Ver. Acc.*** *[m/s²]*	***Improvement (%)***	$c_{\min,front}$ [N.s/m]	$c_{max,front}$ [N.s/m]
No Control (Passive)	0.2236	-	3081.60	3081.60
Semi-active on/off	0.1920	14.13	1028.60	5167.60
Skyhook Continuous	0.1906	14.76	1028.60	4393.10

Table 18

RMS of Vertical Acceleration and Optimized Parameters for Suspension Control over Half Car of VAN EV Light Duty Vehicle Passing over Speed Bump for Rear Axle

Suspension System	***RMS of Ver. Acc.*** *[m/s²]*	***Improvement (%)***	$c_{min,rear}$ [N.s/m]	$c_{max,rear}$ [N.s/m]
No Control (Passive)	0.2236	-	5432.64	5432.64
Semi-active on/off	0.1916	14.31	5421.40	13115.00
Skyhook Continuous	0.1887	15.61	5398.50	11745.00

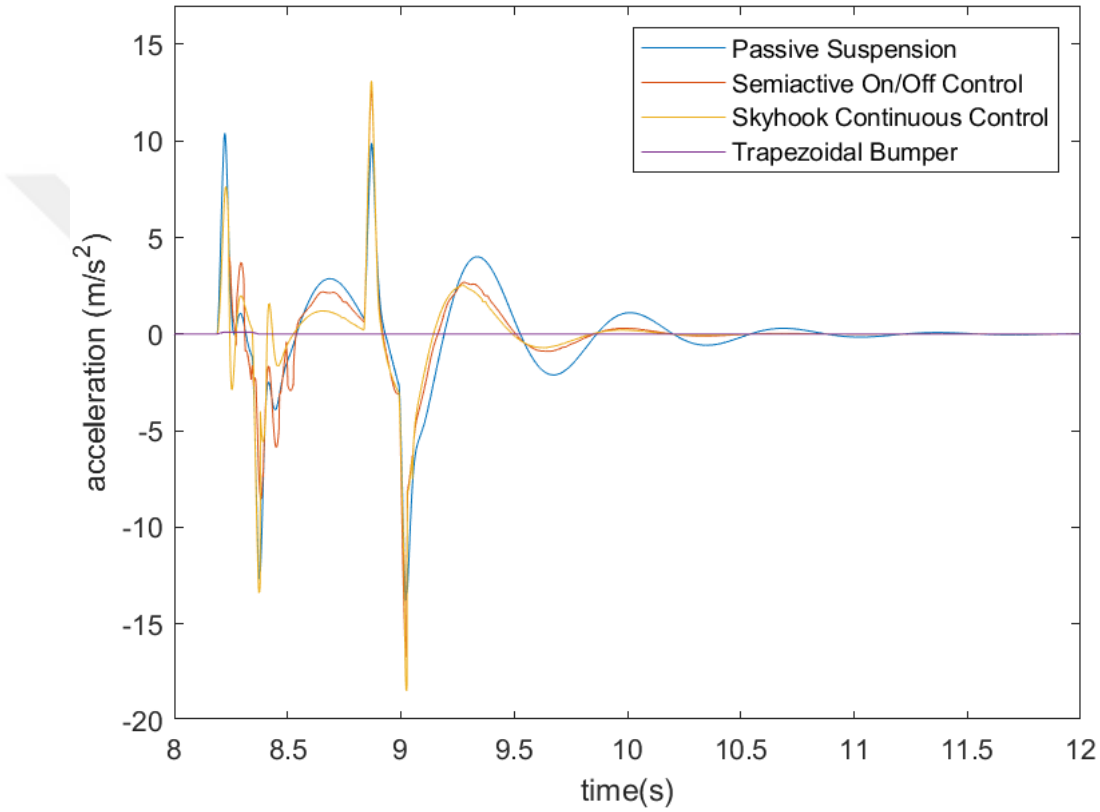

Figure 45 Half-car vertical acceleration performance comparison among the considered suspensions for the VAN EV over a speed bump.

According to vertical acceleration performance comparison demonstrated in *Figure 45* and the RMS values given in Table 16, Table 17, the skyhook continuous controlled suspension provides better ride comfort.

On the other hand, the displacement performance is better in semiactive on/off suspension as can be seen in *Figure 46* below because PSO is performed based on the minimization of the RMS of acceleration at front left portion of the vehicle.

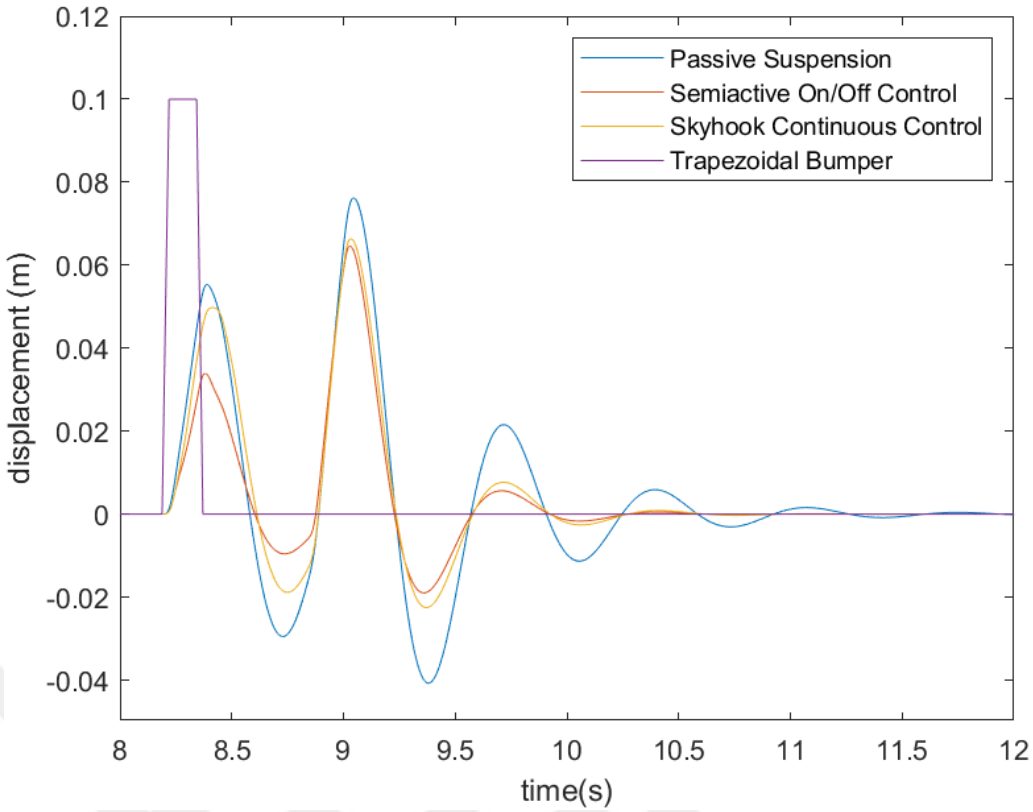

Figure 46 Half-car vertical displacement performance comparison among the considered suspensions for the VAN EV over a speed bump.

Similar to the speed bumper, according to vertical acceleration performance comparison in *Figure 47* and the RMS values in Table 18 and Table 19, the skyhook continuous controlled suspension gives better results.

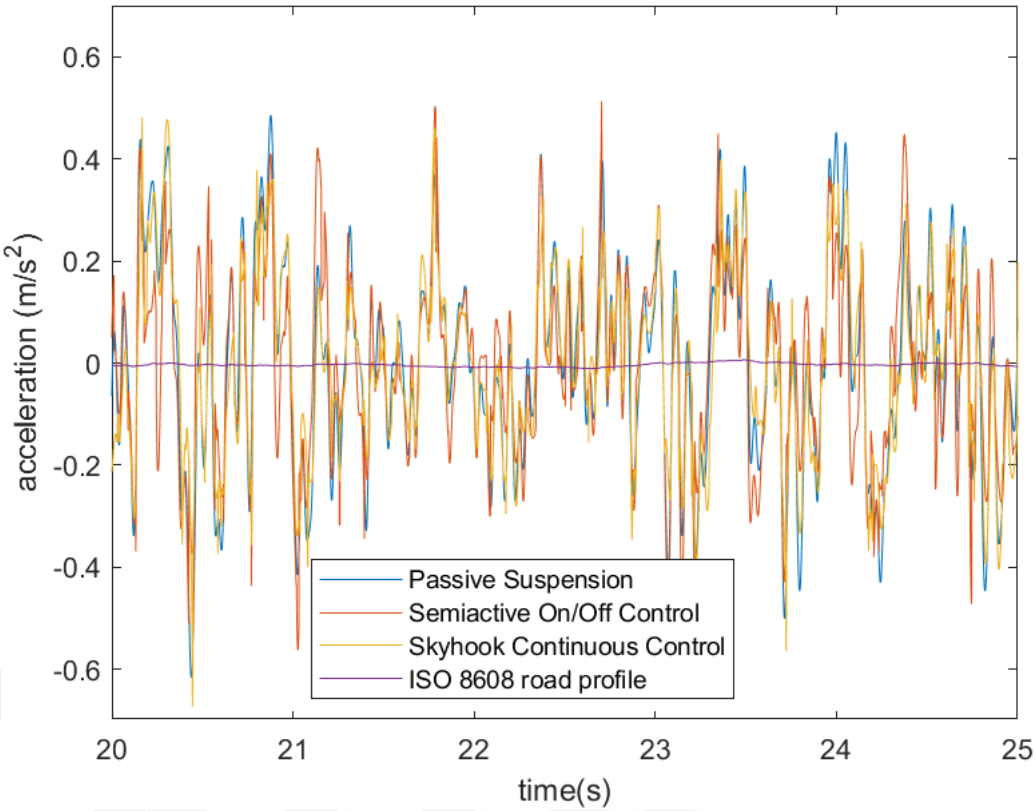

Figure 47 Half-car vertical acceleration performance comparison among the considered suspensions for the VAN EV over a ISO8608 road profile.

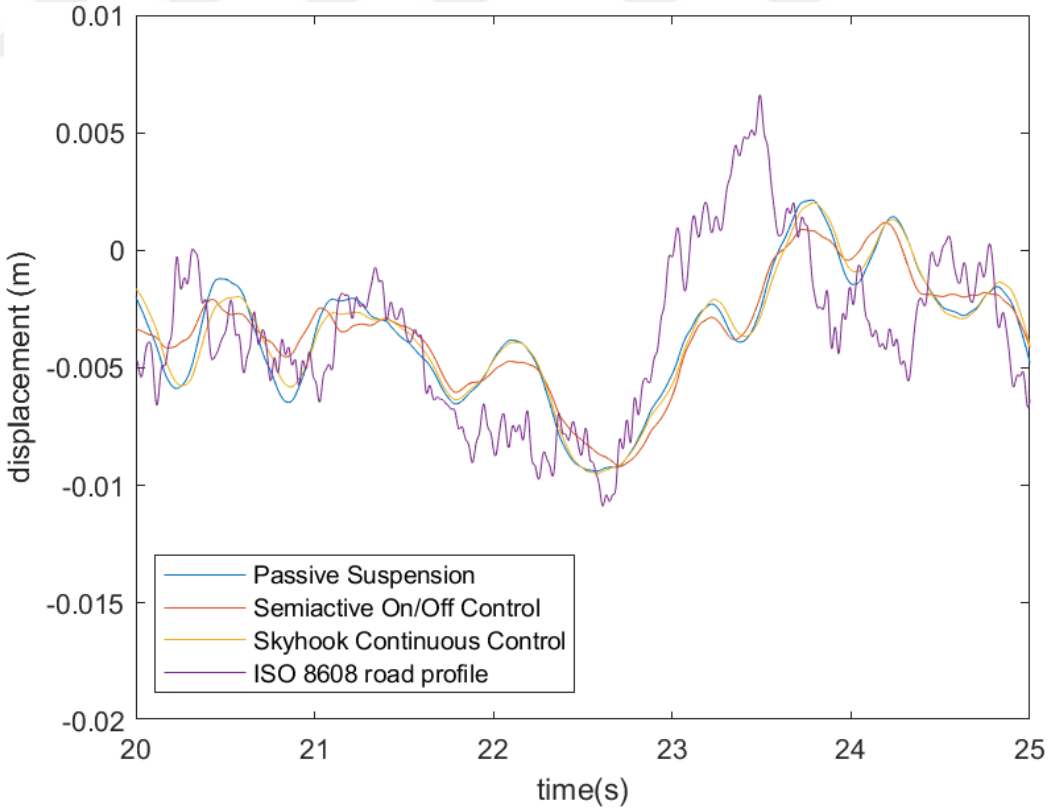

Figure 48 Half-car vertical displacement performance comparison among the considered suspensions for the VAN EV over a ISO8608 road profile.

Considering the same motivation of the study performed for the passenger car, we utilize the VSM full car model of VAN EV to see the dynamic behaviour of considered suspension system control performances with physical vehicle model nonlinearities. This way, performance comparison which is more accurate to the real-world case is assessed as compared to the simplified quarter and half car models in Simulink. VSM simulations reveal lower RMS values for controlled suspensions over bumper as can be seen in *Table 20* and *Figure 49* where the continuous skyhook control provides the lowest RMS of vertical acceleration. This result is consistent with the results for compact Sedan car given in Section 5.3.3 and the reason behind this result is same with the explanations made for the compact Sedan.

Table 19

RMS of Vertical Acceleration for Suspension Control of VAN EV Light Duty Passing over Speed Bumper and ISO 8608 Road Profile for AVL VSM Model

Suspension System	***RMS of ISO 8608 Ver. Acc.*** *[m/s²]*	***Improvement on ISO 8608***	***RMS of Speed Bumper Ver. Acc.*** *[m/s²]*	***Improvement on Speed Bump***
No Control (Passive)	0.3313	-	1.9922	-
Semi-active on/off	0.3237	2.29	1.6467	17.34
Skyhook Continuous	0.3234	2.38	1.6323	18.06

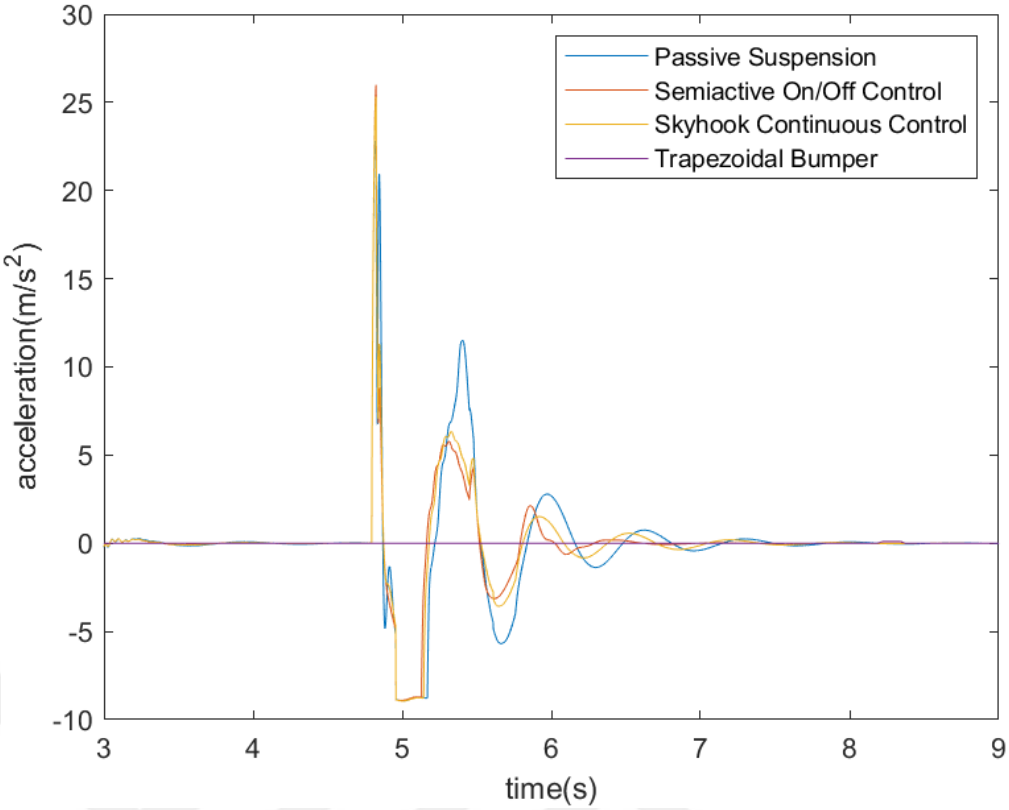

Figure 49 VSM Full-car vertical acceleration performance comparison among the considered suspensions for the VAN EV over a speed bump.

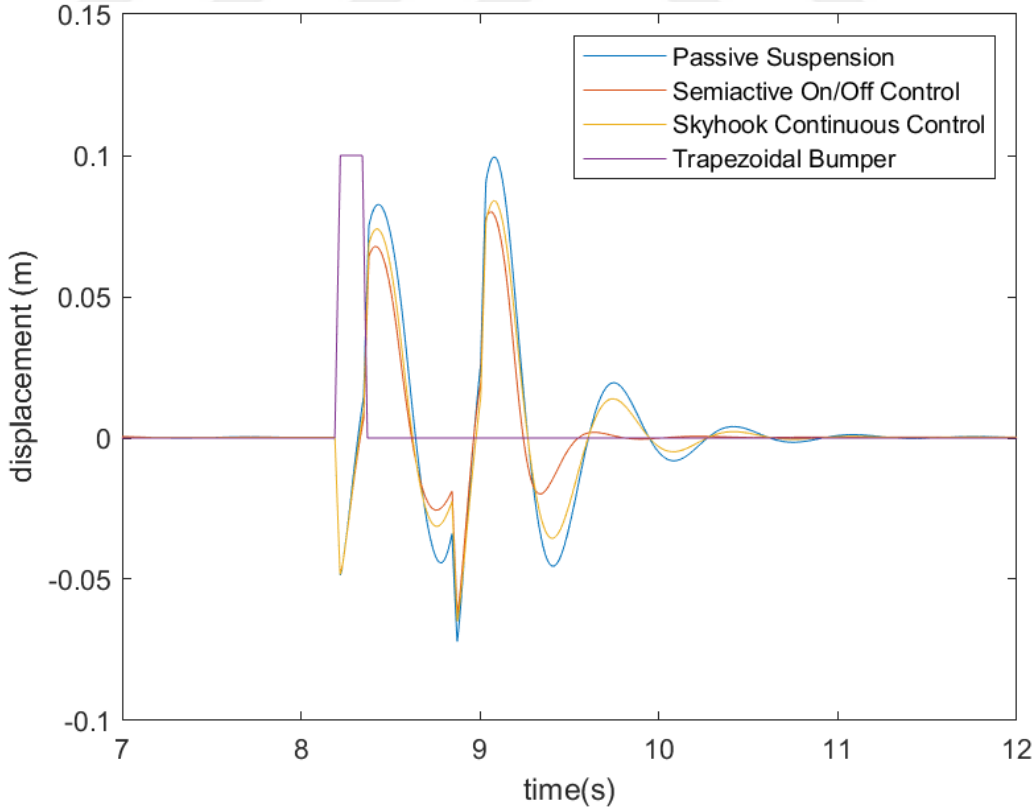

Figure 50 VSM Full-car vertical displacement performance comparison among the considered suspensions for the VAN EV over a speed bump.

According to Table 20 and *Figure 51*, the skyhook continuous controlled suspension behaviour is also the best over semi-active on/off and passive suspensions for ISO 8608 random road profile. The vertical displacement of vehicle is not in parallel with accelerations. This is because PSO is conducted based on RMS acceleration values.

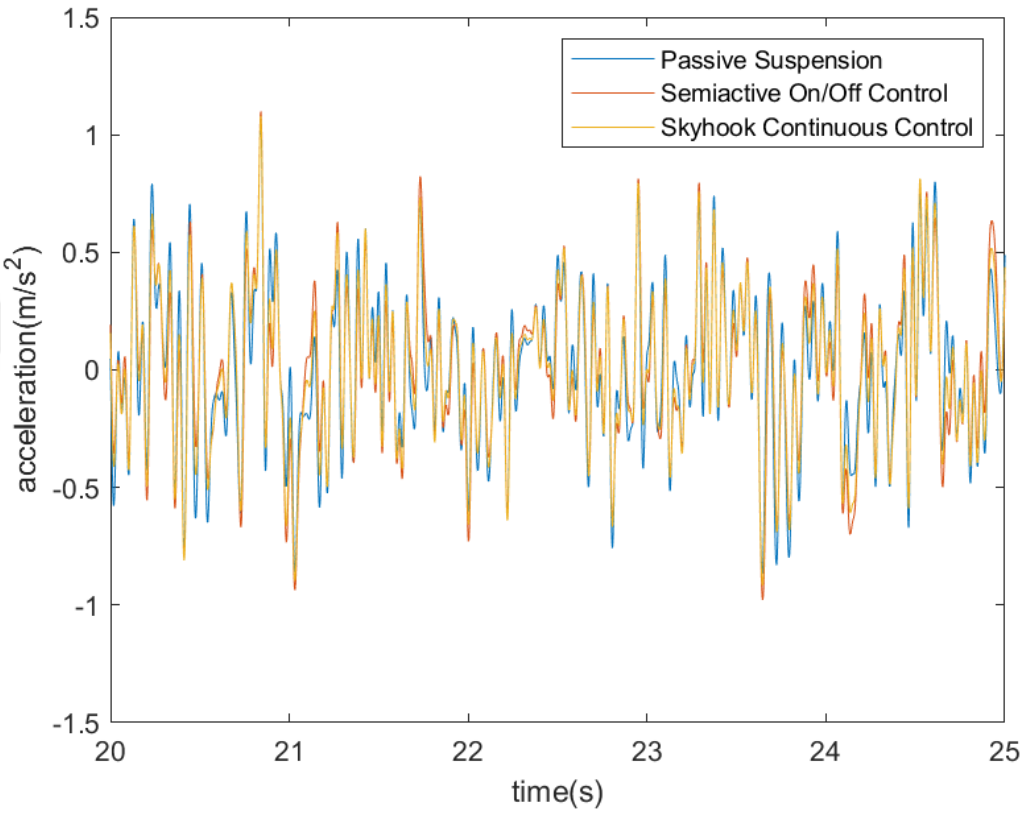

Figure 51 VSM Full-car vertical acceleration performance comparison among the considered suspensions for the VAN EV over a ISO8608 road profile.

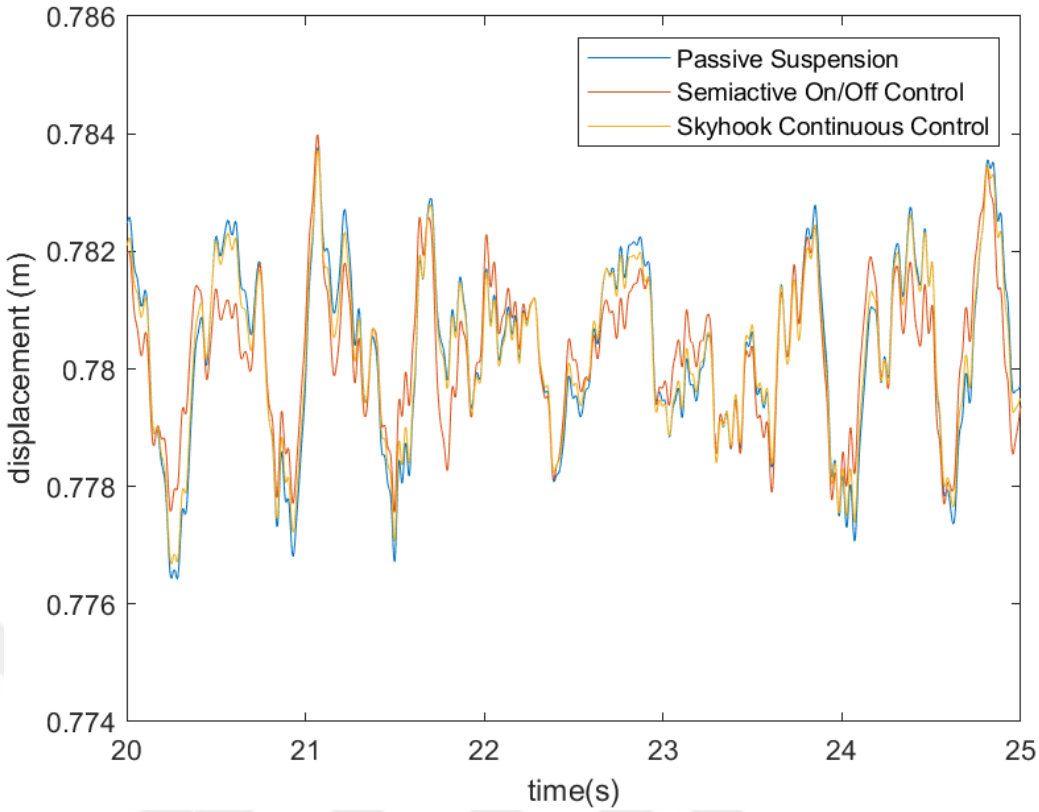

Figure 52 VSM Full-car vertical displacement performance comparison among the considered suspensions for the VAN EVs over a ISO8608 road profile.

Chapter 6

Discussions and Conclusions

In this thesis, there are two semi-active suspension control strategies which are skyhook continuous and on/off control examined in two different random road disturbance scenarios. Compact class passenger and light duty commercial vehicles are used to implement the proposed semi-active control strategies. The control laws for the semi-active suspension are parametrized through simulation-based optimization adapting the PSO algorithm where the RMS of the vehicles vertical acceleration is used as a measure of the ride comfort. The damping coefficient parameter limits are determined to minimize the RMS of the vehicle vertical acceleration. To the best of our knowledge, it is the first time to utilize PSO algorithm for parametrization of the considered semi-active suspension controls. Also, the utilized approach is implemented for vehicles with unidentical front and rear axis suspensions, namely for a light duty VAN EV.

There are two considered road disturbance scenarios: the vehicle passing over a standard speed bumper and the vehicle moving on a standard road profile. These scenarios are realized through simulations with appropriate road inputs to the vehicle models created in both MATLAB Simulink and AVL VSM vehicle dynamic tool. The optimal suspension control parameterization is performed by implementing PSO algorithm based on the simplified linear quarter and half car simulation models. To see the almost real-world impact of the parametrized controllers, the semi-active suspension systems are implemented in AVL VSM tool which provides simulations based on interconnection of whole vehicle components/ parts realized by rigid bodies with Simscape Multibody library. The aim is also to see the responsive behaviour of the controllers in linear and nonlinear vehicle models under constant vehicle speeds and to compare the model effects. The performances of the semi-active suspension controls are compared with the passive suspension system and the improvement on the ride comfort is assessed through the suspension control types, vehicle types and road disturbance scenarios. Based on the performed study, the followings are concluded and observed:

- Optimal suspension control parametrization depends on the road disturbance, i.e. road scenario, and the simulation-based optimization results in different control parameters for different scenarios to achieve the best ride comfort. Thus, we conclude that the preview-based suspension control is useful to improve the ride comfort and the approach performed in this thesis may be utilized for such purposes.
- The ride comfort attained by the suspension control parametrized through linear models is observed when applied to a more realistic nonlinear model in AVL VSM tool. However, the followings are remarked:
    - Nonlinearities in real world vehicle especially related to tire dynamics and suspension kinematics play a crucial role in absorbing random road disturbances caused by secondary road profile (ISO 8608 Class B medium-frequency vibration). In fact, semiactive controllers do not create considerable performance improvements over this profile.
    - Standard bumper has impact harshness effects on vehicle. Therefore, semiactive controllers provide considerable amount of ride comfort enhancements.
    - Parameter optimization is required to be done over half car vehicle models for which the vehicles have non-identical suspensions for front and rear axles
- The effort on compact class vehicle shows that controlled suspension design can be done over linear models especially over impact harshness road inputs for preventing overengineering.
- Skyhook continuous control does not have considerable effect for commercial VAN EV when it is compared with semi active on/off suspension when the control parameters are optimized with the proposed approach ..
- The overshoots observed in vertical acceleration and displacement for skyhook continuous control on AVL VSM model have amplitude less than the ones observed for on/off control law when compared with simulations performed through simplified linear models. We think this is due to the switching characteristics of the on/off control which increases hard nonlinearities together with real vehicle dynamics.

REFERENCES

Agostinacchio, M., Ciampa, D., & Olita, S. (2014). The vibrations induced by surface irregularities in road pavements - a Matlab® approach. *European Transport Research Review*, *6*(3), 267–275. https://doi.org/10.1007/s12544-013-0127-8

Ahmadian, M. (2001). ACTIVE CONTROL OF VEHICLE VIBRATION. In *Encyclopedia of Vibration* (pp. 37–45). Elsevier. https://doi.org/10.1006/rwvb.2001.0193

Alciatore, D. G., & Histand, M. B. (2012). *Introduction to mechatronics and measurement systems*. McGraw-Hill.

Allied Market Research. (2023). Automotive suspension market size, trend, manufacturer, share. Retrieved from https://www.alliedmarketresearch.com

AVL VSM 2021TM Efficient driving pleasure AVL VSMTM Offline Real Time Vehicle Dynamics Simulation. (2021).

BS 6841:1987 Guide to measurement and evaluation of human exposure to whole-body mechanical vibration and repeated shock. (n.d.). https://www.en-standard.eu. https://www.en-standard.eu/bs-6841-1987-guide-to-measurement-and-evaluation-of-human-exposure-to-whole-body-mechanical-vibration-and-repeated-shock/

Cao, D., Song, X., & Ahmadian, M. (2011). Editors' perspectives: Road vehicle suspension design, dynamics, and control. *Vehicle System Dynamics*, *49*(1–2), 3–28. https://doi.org/10.1080/00423114.2010.532223

Chen, S., He, R., Liu, H., & Yao, M. (2012). Probe into necessity of active suspension based on LQG control. *Physics Procedia*, *25*, 932-938. https://doi.org/10.1016/j.phpro.2012.03.180

Dacova, D. (2021). Ride comfort in road vehicles: A literature review. *International Scientific Journal "TRANS & MOTAUTO WORLD,"* 6(2), 65-69.

De Bruyne, S., Van der Auweraer, H., Anthonis, J., Desmet, W., & Swevers, J. (2012). Preview control of a constrained hydraulic active suspension system. In Proceedings of the 51st IEEE Conference on Decision and Control (pp. 4400-4405). IEEE. https://doi.org/10.1109/CDC.2012.6426153

Drehmer, L. R. C., Paucar Casas, W. J., & Gomes, H. M. (2015). Parameters optimisation of a vehicle suspension system using a particle swarm optimisation algorithm. Vehicle System Dynamics, 53(4), 449–474. https://doi.org/10.1080/00423114.2014.1002503

ElMadany, M. M., & Abduljabbar, Z. S. (1999). Linear Quadratic Gaussian control of a quarter-car suspension. *Vehicle System Dynamics: International Journal of*

Vehicle Mechanics and Mobility, *32*(6), 479-497. https://doi.org/10.1076/vesd.32.6.479.4224

Fukuda, T., Zhang, X., Hasegawa, Y., Matsumoto, T., & Hoshino, H. (2004). Preview posture control and impact load control of rough terrain vehicle with interconnected suspension. In *Proceedings of the 2004 IEEE/RSJ International Conference on Intelligent Robots and Systems (IROS 2004)* (pp. 761-766). IEEE.

Genta, G., & Morello, L. (2020). *The automotive chassis: Volume 1: Components design* (2nd ed.). Springer. https://doi.org/10.1007/978-3-030-35635-4

Goenaga, B., Fuentes, L., & Mora, O. (2017). Evaluation of the methodologies used to generate random pavement profiles based on the power spectral density: An approach based on the international roughness index. *Ingeniería e Investigación*, *37*(1), 49–57. https://doi.org/10.15446/ing.investig.v37n1.57277

Gołdasz, J., & Dzierzek, S. (2016). Parametric study on the performance of automotive MR shock absorbers. *IOP Conference Series: Materials Science and Engineering*, *148*(1). https://doi.org/10.1088/1757-899X/148/1/012004

ISO 2631-1:1997. (1997, June 1). ISO. https://www.iso.org/standard/7612.html

KARNOPP Professor, D., & CROSBY Program Development Manager R A HARWOOD, M. J. (1974). *Vibration Control Using Semi-Active Force Generators*. https://manufacturingscience.asmedigitalcollection.asme.org

Kaldas, M., Caliskan, K., Henze, R., & Küçükay, F. (2014). Preview Enhanced Rule-Optimized Fuzzy Logic Damper Controller. SAE International Journal of Passenger Cars - Mechanical Systems, 7(2), 804–815. https://doi.org/10.4271/2014-01-0868

Kennedy, J., Eberhart, R., & gov, bls. (n.d.). *Particle Swarm Optimization*.

Kırbaş, U., & Karaşahin, M. (2023). Karayolu-demiryolu hemzemin geçitlerinde maruz kalınan titreşimin insan sağlığını etkileme seviyeleri Human health impact levels of vibration exposure at highway-railroad level crossings. *Bilim. Derg. / NOHU J. Eng. Sci*, *12*(2), 487–500. https://doi.org/10.28948/ngmuh.1214112

Liu, C., Chen, L., Yang, X., Zhang, X., & Yang, Y. (2019). General Theory of Skyhook Control and its Application to Semi-Active Suspension Control Strategy Design. *IEEE Access*, *7*, 101552–101560. https://doi.org/10.1109/ACCESS.2019.2930567

Liu, C., Chen, L., Lee, H. P., Yang, Y., & Zhang, X. (2023). Generalized Skyhook-Groundhook Hybrid Strategy and Control on Vehicle Suspension. *IEEE Transactions on Vehicular Technology*, *72*(2), 1689–1700. https://doi.org/10.1109/TVT.2022.3210171

Mo, C., & Sunwoo, M. (2002). A semiactive vibration absorber (SAVA) for automotive suspensions. *International Journal of Vehicle Design*, *29*(1–2), 83–95. https://doi.org/10.1504/IJVD.2002.002002

Morato, M. M., Nguyen, M. Q., Sename, O., & Dugard, L. (2019). Design of a fast real-time LPV model predictive control system for semi-active suspension control of a full vehicle. *Journal of the Franklin Institute*, *356*(3), 1196–1224. https://doi.org/10.1016/j.jfranklin.2018.11.016

OEM Off-Highway. (2024). Reducing weight and improving suspension performance. Retrieved from https://www.oemoffhighway.com

Park, S., Popov, A. A., & Cole, D. J. (2004). Influence of soil deformation on off-road heavy vehicle suspension vibration. *Journal of Terramechanics*, *41*(1), 41–68. https://doi.org/10.1016/j.jterra.2004.02.010

Rajamani, R. (2012). Vehicle dynamics and control (2nd ed.). Springer. https://doi.org/10.1007/978-1-4614-1433-9

Rossi, C., & Lucente, G. (2004). H∞ control of automotive semi-active suspensions. In *Proceedings of the IFAC Advances in Automotive Control Conference* (pp. 559-564). Elsevier.

Rusli, F. Z., & Darsivan, F. J. (2019). The effect of hydraulic damper characteristics on the ride and handling of ground vehicle. *International Journal of Recent Technology and Engineering (IJRTE), 7*(6S), 113-118. https://www.legislation.gov.uk/uksi/1999/1025

Salmani, H., Abbasi, M., Fahimi Zand, T., Fard, M., & Nakhaie Jazar, R. (2022). A new criterion for comfort assessment of in-wheel motor electric vehicles. *JVC/Journal of Vibration and Control*, *28*(3–4), 316–328.

Sam, Y. M., & Hudha, K. (2006). Modelling and force tracking control of hydraulic actuator for an active suspension system. In *Proceedings of the 2006 IEEE International Conference on Industrial Electronics and Applications (ICIEA 2006)* (pp. 1-6). IEEE. https://doi.org/10.1109/ICIEA.2006.257658

Savaresi, S. M., & Silani, E. (2004). On the optimal predictive control algorithm for comfort-oriented semi-active suspensions. In *Proceedings of the 2004 SAE Automotive Dynamics, Stability & Controls Conference* (SAE Technical Paper 2004-01-2088). Society of Automotive Engineers. https://doi.org/10.4271/2004-01-2088

Savaresi, S. M., Poussot-Vassal, C., Spelta, C., Sename, O., & Dugard, L. (2010). Semi-Active Suspension Technologies and Models. In *Semi-Active Suspension Control Design for Vehicles* (pp. 15–39). Elsevier. https://doi.org/10.1016/b978-0-08-096678-6.00002-x

Sename, O. (2021). Review on LPV approaches for suspension systems. *Electronics, 10*(17), 2120. https://doi.org/10.3390/electronics10172120

Soliman, A. M. A., & Kaldas, M. M. S. (2021). Semi-active suspension systems from research to mass-market – A review. *Journal of Low Frequency Noise Vibration and Active Control, 40*(2), 1005–1023. https://doi.org/10.1177/1461348419876392

Song, S., & Wang, J. (2020, August 28). *Incremental Model Predictive Control of Active Suspensions with Estimated Road Preview Information from a Lead Vehicle*. Journal of Dynamic Systems Measurement and Control-transactions of the Asme. https://doi.org/10.1115/1.4047962

Sharkawy, A. (2005). Adaptive fuzzy control of active suspension systems. *Journal of Engineering and Applied Science, 52*(4), 779-795.

Sharp, R. S., & Peng, H. (2011). Vehicle dynamics applications of optimal control theory. *Vehicle System Dynamics, 49*(7), 1073-1111. https://doi.org/10.1080/00423114.2011.586707

Shihabudheen, K. v., Mahesh, M., & Pillai, G. N. (2018). Particle swarm optimization based extreme learning neuro-fuzzy system for regression and classification. Expert Systems with Applications, 92, 474–484. https://doi.org/10.1016/j.eswa.2017.09.037

Skogestad, S., & Postlethwaite, I. (2005). *Multivariable feedback control: Analysis and design* (2nd ed.). John Wiley & Sons.

Streiter, R. Active preview suspension system. ATZ Worldw 110, 4–11 (2008). https://doi.org/10.1007/BF03225003

Tharehalli mata, G., Mokenapalli, V., & Krishna, H. (2021). Performance analysis of MR damper based semi-active suspension system using optimally tuned controllers. Proceedings of the Institution of Mechanical Engineers, Part D: Journal of Automobile Engineering, 235(10–11), 2871–2884. https://doi.org/10.1177/09544070211004467

The Secretary of State for the Environment, Transport and the Regions. (1999, April 28). *Highways (Road Humps) Regulations*. legislation.gov.uk.

Theunissen, J., Tota, A., Gruber, P., Dhaens, M., & Sorniotti, A. (2021). Preview-based techniques for vehicle suspension control: a state-of-the-art review. In *Annual Reviews in Control* (Vol. 51, pp. 206–235). Elsevier Ltd. https://doi.org/10.1016/j.arcontrol.2021.03.010

Tseng, H. E., & Hrovat, D. (2015). State of the art survey: Active and semi-active suspension control. *Vehicle System Dynamics: International Journal of Vehicle Mechanics and Mobility*. https://doi.org/10.1080/00423114.2015.1037313

Umar, R. (2014). Hybrid cooperative energy detection techniques in cognitive radio networks. In *Chapter of an Unpublished Manuscript*. Retrieved from https://www.researchgate.net/publication/266614526_Hybrid_Cooperative_Energy_Detection_Techniques_in_Cognitive_Radio_Networks

Yang, A.; Zang, Y.; Xu, L.; Li, L.; Tan, D. A Systematic Review and Future Development of Automotive Chassis Control Technology. Appl. Sci. 2023, 13, 11859. https://doi.org/10.3390/app132111859

Yu, H., & Yu, N. (2003). Application of genetic algorithms to vehicle suspension design. *Project Report, Department of Mechanical Engineering, Pennsylvania State University*.

Yun, S.; Lee, J.; Jang, W.; Kim, D.; Choi, M.; Chung, J. Dynamic Modeling and Analysis of a Driving Passenger Vehicle. Appl. Sci. 2023, 13, 5903. https://doi.org/10.3390/app13105903

Zhang, J., Long, F., Lin, J., & Zhu, X. (2024). Particle swarm optimized fuzzy proportional-integral-derivative controller-based transverse leaf spring active suspension for vibration control. Journal of Low Frequency Noise Vibration and Active Control, 43(2), 979–996. https://doi.org/10.1177/14613484231221953

Zhuo, L., Cheng, Z., Wang, Y., & Liu, L. (2018). Design of vehicle trajectory optimization based on multiple-shooting method and modified particle swarm optimization. In *Proceedings of the 37th Chinese Control Conference* (pp. 4649-4654). Wuhan, China.

Wang, L., Lv, Z., & Li, Q. (2015). Road friendliness optimization of heavy vehicle suspension based on particle swarm algorithm. In Proceedings of the 4th International Conference on Computer, Mechatronics, Control and Electronic Engineering (ICCMCEE 2015) (pp. 1328-1333). Atlantis Press.